Stony Brook University

OFFICIAL COPY

The official electronic file of this thesis or dissertation is maintained by the University Libraries on behalf of The Graduate School at Stony Brook University.

© All Rights Reserved by Author.

Molecular Origin of Polymer Film Stability on Solid Substrates

A Thesis Presented

by

Jiaxun Wang

to

The Graduate School

in Partial Fulfillment of the

Requirements

for the Degree of

Master of Science

in

Materials Science and Engineering

Stony Brook University

December 2014

Stony Brook University

The Graduate School

Jiaxun Wang

We, the thesis committee for the above candidate for the
Master of Science degree, hereby recommend
acceptance of this thesis.

Tadanori Koga – Thesis Advisor
Associate Professor, Department of Materials Science and Engineering

Jonathon Sokolov – Second Reader
Professor, Department of Materials Science and Engineering

T. A. Venkatesh – Third Reader
Associate Professor, Department of Materials Science and Engineering

This thesis is accepted by the Graduate School
Charles Taber
Dean of the Graduate School

Molecular Origin of Polymer Film Stability on Solid Substrates

by

Jiaxun Wang

Master of Science

in

Materials Science and Engineering

Stony Brook University

2014

Abstract

Despite intensive studies over the last 20 years, the nature of wetting/dewetting of ultrathin polymer films (i.e., thickness less than 100 nm) on impenetrable solid surfaces still remains unsolved. We report that stabilization of liquid polymer films on solids can be controlled by nanoscale architectures of polymer chains adsorbed on the solid surfaces. A series of monodisperse PS ultrathin films (20 nm in thickness) with different molecular weights (Mw) were prepared on silicon (Si) substrates with a natural amorphous Si dioxide layer. The PS thin films were annealed at high temperatures, and the film stability was studied by combining optical and atomic force microscopes. At the same time, the annealed PS films were further leached with a good solvent and the residue films (several nanometers thick) were characterized by ellipsometry and X-ray photoelectron spectroscopy. We found that the film stability is attributed to the wetting-dewetting transition at the interface between the free polymer chains and adsorbed polymer chains. The present findings provide a simple and effective alternative in place of

conventional end-grafting approach, by modifying the substrate surfaces with the chemically identical polymer chains bound to solids via physisorption.

Table of Contents

Abstract iii

Table of Contents v

List of Figures vii

List of Schemes xii

Acknowledgments xiv

Chapter 1 Introduction 1

1.1 Thermodynamic Stability or instabilities of the polymer thin films on top of a solid 1

1.2 Patterns formation by dewetting of polymer thin film 4

1.3 Influence of native dioxide layer on the dewetting of polymer thin films 8

1.4 Adsorption of polystyrene at polymer/substrate interface 10

1.5 Dewetting at a polymer-polymer interface 14

Chapter 2 Experimental Section 16

2.1 Sample Preparation 16

2.2 Atomic Force Microscope (AFM) measurements. 18

2.3 Optical Microscope (OM) Measurements. 18

Chapter 3 Result and discussion 20

3.1 Molecular weight dependence of polystyrene films on silicon substrates. 20

3.2 How molecular weight affect the formation of adsorbed layer near the substrates interface? 22

3.3 Correlation between chain adsorption and the dewetting of polystyrene films. 26

3.4 The role of the flattened layer and loosely adsorbed layer. ... 28

3.5 What happens if the thickness of the PS films become very small? ... 36

3.6 The mechanism of wetting/ dewetting of thin polymer films on silicon substrate. ... 39

Chapter 4. Conclusion ... 42

References ... 43

List of Figures

Figure 1. A sketch of a liquid drop on top of a solid substrate. (a) Complete wetting is characterized by a contact angle $\theta = 0$, (b) partial wetting by $0 < \theta < \pi$, and (c) non-wetting by $\theta = \pi$.[6] 2

Figure 2. Long range (characterized by the Hamaker constant A) and short range (characterized by the spreading coefficient S) intermolecular interactions in thin films. (a) Schematic drawing intended to show the force acting on a thin film (thickness h) of liquid 3 on substrate 1 and bounded by the surrounding (deformable) medium 2. (b) Variations of the excess free energy per unit area (ΔG) with film thickness (h) for positive (repulsive) and negative (attractive) A, respectively. Attractive forces try to reduce the thickness h (they destabilize the film), while repulsive forces try to increase it (they stabilize the film). Modifying the substrate by grafting a polymer brush adds a short-ranged stabilizing effect.[10] 3

Figure 3. In thin films, attractive long-range interactions cause the amplification of capillary waves of amplitude A_0, eventually leading to film rupture at a characteristic wavelength λ. Both, λ and the rupture time τ depend significantly on the film thickness.[10] 4

Figure 4. Pictures series taken by a light microscope: a 80 nm thick polystyrene film of 65 kg/mol molecular weight is dewetting at 135°C from a hydrophobized silicon substrate for approximately (from left to right) 2 min, 10 min, 30 min, and 100 min.[12] 5

Figure 5. Effective interface potential $\varphi(h)$ as a function of film thickness h for stable (1), unstable (2), and metastable (3) films. [11] 6

Figure 6. (a–c) AFM images of dewetting PS (2k) films. Scale bars indicate 5 μm, z-scale ranges from 0 nm (black) to 20 nm (white): (a) spinodal dewetting of 3.9 nm PS on type C wafer. The inset shows a Fourier transform of the image. (b) Thermal nucleation dewetting of 4.1 nm PS on type B wafer. (c) Heterogeneous nucleation dewetting of 6.6 nm PS on a type B wafer.[11] 7

Figure 7. Long-range part of the effective interface potential φ(h) as function of PS film thickness h for different SiO_x layer thickness ranging from 0 nm (dotted line) to infinity (solid line), calculated with the formula given in Eq. (10). The Hamaker constants were calculated from the optical constants of the involved materials.[12] 9

Figure 8. Stability diagram of PS films on top of Si wafers with variable oxide layer thickness.[12] 10

Figure 9. Annealing time dependence of the thickness of the residual film, $h_{residue}$, obtained for PS (M_W 1⁄4 44.1 kDa)/H-Si (solid symbols) and bare H-Si (open symbols). The annealing was performed at T1⁄41501C in air. Figure reproduced from Fujii et al.[67] with permission from the American Chemical Society.[27] 11

Figure 10. Desorption kinetics of the equilibrium adsorbed PS (Mw= 170 kDa) layer during the toluene leaching. The inset shows the schematic view of the two different chain conformations.[22] 13

Figure 11. OM images of 20 nm-thick PS films with five different M_w, 3.68 kDa (a, f), 13.1 kDa (b, g), 30 kDa (c, h), 50 kDa (d, i) and 123 kDa (e, j) on bare H-Si (a-e) and SiO_x/Si (f-j) substrates after thermally annealed at 150 ºC under vacuum for 9 days. The insets in (a), (b), (f) and (g) are the OM images with a smaller magnification of the same sample. The nanoscale

surface morphologies (AFM images) of the dewetted regions in (a-d) and (f-i) were shown in (k-n) and (o-r), respectively. The height scale for the AFM images is 0 – 10 nm. 21

Figure 12. Thicknesses of the residual PS layers on H-Si and SiO_x/Si substrates as a function of M_w after leaching with toluene (lower desorption energy) or chloroform (higher desorption energy). The original PS films (20 nm-thick) were thermally annealed at 150 ºC under vacuum for 9 days before the leaching process. 23

Figure 13. The surface morphologies of the residual PS layers on H-Si and SiO_x/Si substrates as a function of M_w after leaching with toluene (lower desorption energy) and/or chloroform (higher desorption energy). The original PS films (20 nm-thick) were thermally annealed at 150 ºC under vacuum for 9 days before the leaching process. The height scale for the AFM images is 0 – 10 nm. 24

Figure 14. X-ray photoelectron spectroscopic C 1s narrow scan of the residual film obtained from 30 kDa PS flattened layer on H-Si after annealing at 150 ºC for 9 days followed by thorough rinsing in chloroform. 25

Figure 15. (a) show AFM images of 5 nm-thick PS 30K films on H-Si substrate. The original PS films were thermally annealed at 150ºC under vacuum for 9 days. The surface morphologies of the dewetted region in (a) were shown in (b). The height scale for the AFM images is 0-10nm. 27

Figure 16. (a-e) shows OM images of 20 nm-thick PS films with five different M_w, 3.68 kDa (a), 13.1 kDa (b), 30 kDa (c), 50 kDa (d) and 123 kDa (e) on PS flattened layer (M_w = 650 kDa) modified H-Si substrate after thermally annealed at 150 ºC under vacuum for 9 days. (f-i) shows OM images of 20 nm-thick PS films with two different M_w, 3.68 kDa (f, g) and 50 kDa (h, i) on

PS loosely adsorbed layer (M_w = 650 kDa) modified H-Si (f, h) and SiO_x/Si (g, i) substrates after thermally annealed at 150 ºC under vacuum for 9 days. 29

Figure 17. The thicknesses of the residual PS layers on 650K or 50K flattened layer as a function of M_w after leaching with toluene. The original bilayers were thermally annealed at 150 ºC under vacuum for 9 days before the leaching process. 30

Figure 18. The representative static water contact angles of (a) 123kPS flattened layer, (c) 123kPS interfacial sublayer, (d) 20nm-thick 123kPS spin cast film. The representative dynamic water contact angles of 123kPS flattened layer during the advancing and receding process were shown in (d) and (e), respectively. The representative dynamic water contact angles of 123kPS interfacial sublayer during the advancing and receding process were shown in (f) and (g), respectively. 32

Figure 19. (a-d) shows OM images of 20 nm-thick PS films with four different M_w, 3.68 kDa (a), 13.1 kDa (b), 30 kDa (c), 50 kDa (d) on P2VP flattened layer (M_w = 219 kDa) modified SiO_x-Si substrate after thermally annealed at 150 ºC under vacuum for 7 days. (e-h) shows OM images of 20 nm-thick PS films with four different M_w, 3.68 kDa (e), 13.1 kDa (f), 30 kDa (g), 50 kDa (h) on P2VP loosely adsorbed layer (M_w = 219 kDa) modified SiO_x-Si substrates after thermally annealed at 150 ºC under vacuum for 7 days. 34

Figure 20. (a-c) shows AFM images of 5 nm-thick 3.68 kDa PS films on (a) bare H-Si substrate, (b) PS flattened layer (M_w = 650 kDa) modified H-Si substrate and (c) PS loosely adsorbed layer (M_w = 650 kDa) modified H-Si substrate after thermally annealed at 150 ºC under vacuum for 9 days. (d-f) shows AFM images of 5 nm-thick 123 kDa PS films on (d) bare H-Si substrate, (e) PS flattened layer (M_w = 650 kDa) modified H-Si substrate and (f) PS loosely adsorbed layer (M_w =

650 kDa) modified H-Si substrate after thermally annealed at 150 ºC under vacuum for 9 days. The height scale for the AFM images is 0 – 20 nm. 36

List of Schemes

Scheme 1. Sample preparation process used in experiment 16

List of Abbreviations

PS: polystyrene

P2VP: poly(2-vinylpyridine)

AFM: Atomic Force Microscopy

OM: Optical microscope

Acknowledgments

Firstly, I would like to express my deepest appreciation to my thesis advisor, Tadonori Koga, for his unending mentorship and guidance, helping me to hone and enhance my skills as a master's student. His sagacity as my teacher helped make this research and thesis possible. Throughout my research in the lab, he has imbued me with tremendous knowledge and understanding of polymer science which I will be sure to carry with me in my future endeavors.

My thanks also goes out to Naisheng Jiang, a Ph.D student in Professor Koga's lab, who has supported and helped me copiously during my time as a master's student. All my friends support and help are also indispensable throughout my two years study in Stony Brook University.

A heartfelt thanks to my parents, Qingjun Wang and Yaping Liu, for their inexorable patience and gracious support of my master's studies as well as their infinite consideration of my wellbeing at Stony Brook University.

Chapter 1 Introduction

1.1 Thermodynamic Stability or instabilities of the polymer thin films on top of a solid

Thermal stability of thin polymer films against shape changes is of vital importance in both scientific investigations (e.g., adhesion, adsorption, diffusion) and nanotechnological applications such as coatings, dielectric layer, organic photovoltaics and biosensors[1]. Polymer films can be prepared on nonwettable surface by using techniques like spin coating, and such films can either wet or dewet from a solid substrates which depend on several factors including polymer-substrate interfacial energy[2], polarity[3], film thickness[4] and molecular weight[5]. A droplet on a homogeneous surface usually exhibits the form of a spherical cap and the tangent to the droplet at the three phase contact line includes an angle θ with the substrate. Under equilibrium conditions, a given system of solid, liquid, and vapor ate a given temperature and pressure has a unique equilibrium contact angle (θ). The contact angle quantifies the wettability of a solid surface by a liquid via the Young equation:

$$\text{Cos}\theta = (\gamma_{sv} - \gamma_{sl}) / \gamma_{lv} \quad (1)$$

where γ_{sv} and γ_{sl} are the solid/vapor and solid/liquid interfacial free energies, and γ_{lv} is the liquid/vapor surface tension. For $\theta = 0$, a droplet will spread on the substrate. This case is termed complete wetting (Figure 1(a)). For $0 < \theta < \pi$ one speaks of partial wetting (Figure 1(b)), and for $\theta = \pi$ of non-wetting (Figure 1(c)).[6] In other words, the contact angle in Young's equation is determined by the free energies of interfaces between semi-infinite media.

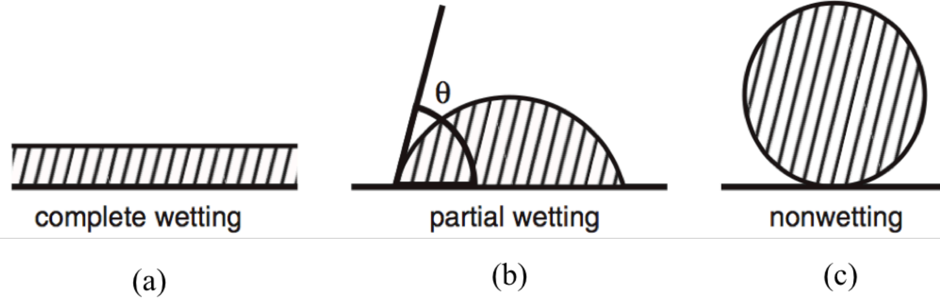

Figure 1. A sketch of a liquid drop on top of a solid substrate. (a) Complete wetting is characterized by a contact angle θ = 0, (b) partial wetting by 0 < θ < π, and (c) non-wetting by θ = π.[6]

In case of wetting, the polymer thin film remained homogeneous and flat with a zero contact angle with the substrate at equilibrium situation. Otherwise, the film would encounter a dewetting process from the initial rupture and growth of holes, coalescence into polygonal network, to the formation of dewetting droplets with clear three phase contact lines and a non-zero contact angle respect to the solid substrates.[7, 8] The polymer thin film wettability is defined by the spreading coefficient. The spreading coefficient(S) is defined from continuum thermodynamics as

$$S = \Delta G = \gamma_{sv} - \gamma_{sp} - \gamma_{pv} \tag{2}$$

Where γ_{sv} and γ_{pv} are the surface free energies of the solid substrate and polymer, respectively, and γ_{sp} is the interfacial free energy between the polymer and the substrate.[9] ΔG is the excess intermolecular interaction free energy which composed of antagonistic (attractive/repulsive) long- and (relatively) short- range interactions, which decay with the local thickness h (Figure 2).

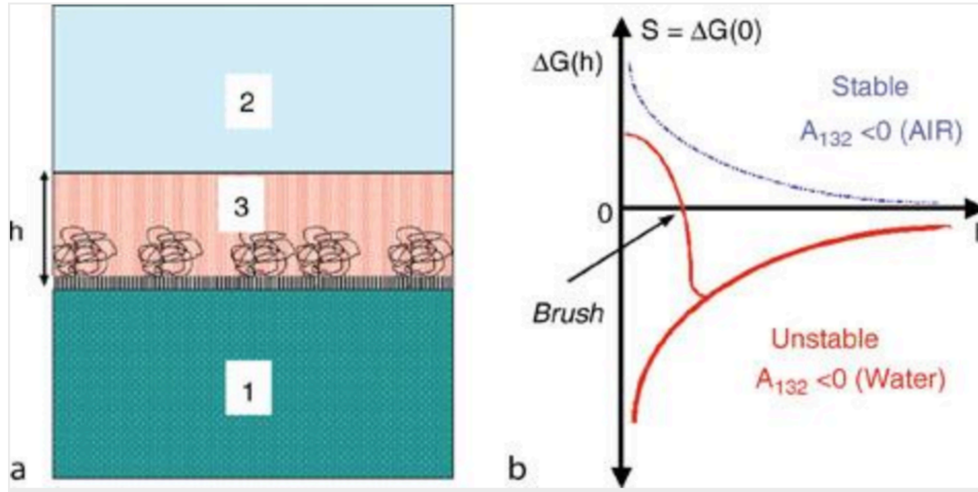

Figure 2. Long range (characterized by the Hamaker constant *A*) and short range (characterized by the spreading coefficient *S*) intermolecular interactions in thin films. (a) Schematic drawing intended to show the force acting on a thin film (thickness *h*) of liquid 3 on substrate 1 and bounded by the surrounding (deformable) medium 2. (b) Variations of the excess free energy per unit area (Δ*G*) with film thickness (*h*) for positive (repulsive) and negative (attractive) *A*, respectively. Attractive forces try to reduce the thickness *h* (they destabilize the film), while repulsive forces try to increase it (they stabilize the film). Modifying the substrate by grafting a polymer brush adds a short-ranged stabilizing effect.[10]

The Hamaker constant A will then give the strength of the van der Waals forces between the two interfaces solid/liquid and liquid/air. If the effective Hamaker *A* is negative, medium 1 and 2 repel each other, seeking to make the film infinitely thick. In the opposite case, positive *A*, the media 1 and 2 attract each other, trying to remove the film completely. Positive *A* also means that a thin film is unstable, as shown in Figure 2. Such attraction then can lead to "roughening" of the film, but the interfacial tension γ will create a Laplace pressure that will smoothen out

undulations, preferentially the ones with a small local radius of curvature. The competition between attractive long-range forces and Laplace pressure thus determines a critical wavelength λ beyond which fluctuations will grow increasingly more rapidly, as shown in Figure 3.

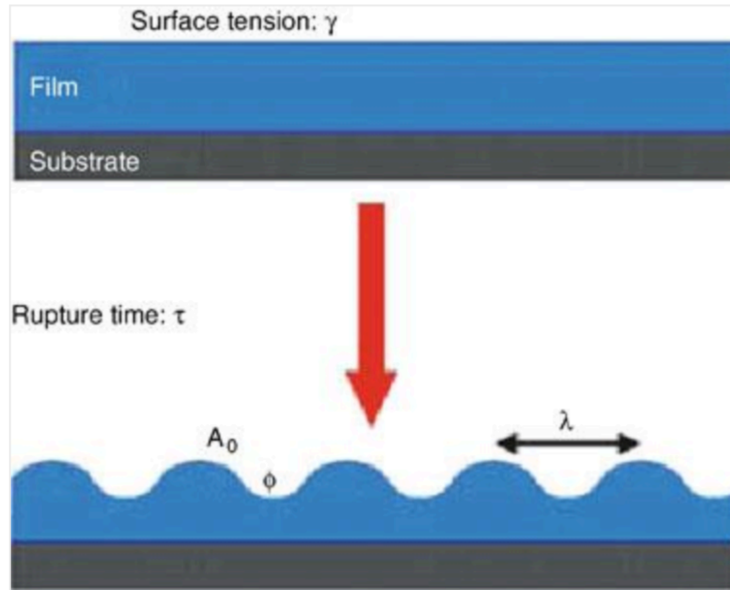

Figure 3. In thin films, attractive long-range interactions cause the amplification of capillary waves of amplitude A_0, eventually leading to film rupture at a characteristic wavelength λ. Both, λ and the rupture time τ depend significantly on the film thickness.[10]

In an approximate theory, the early stages of growth can be described by an exponential function. Eventually, after a time τ, the depressions hit the substrate and, on nonwettable substrates, rupture the film which, in turn, will initiate a dewetting process.[9-11]

1.2 Patterns formation by dewetting of polymer thin film

The process of dewetting can be divided into three stages: in the early stage, holes are generated by a rupture process, as shown in Figure 4(a); in the intermediate stage, the radius of the holes increases, leading to hole coalescence (Figure 4(b- c)). In the intermediate stage, the focus is on the dynamics involved in the dewetting process, its impact on the hole profiles and on its

influence on dewetting patterns. From the dynamics of hole growth as well as from the shape of the liquid rim surrounding the hole one can get information about the slip or no-slip boundary condition of the liquid close to the solid substrate. In the late stage, the straight ribbons that separate two coalescing holes decay into droplets on the substrate.[12]

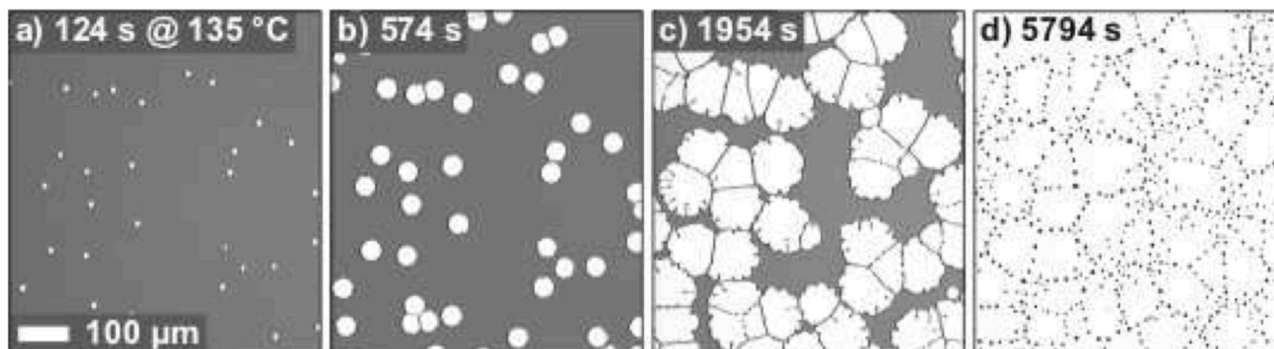

Figure 4. Pictures series taken by a light microscope: a 80 nm thick polystyrene film of 65 kg/mol molecular weight is dewetting at 135°C from a hydrophobized silicon substrate for approximately (from left to right) 2 min, 10 min, 30 min, and 100 min.[12]

A real surface always has some impurities and some defects on it, so it is important to study the dewetting on a hetergeneous surface, where small-scale chemical and/or physical hetergeneities conspire to produce rapid formationof holes locally. Dewetting of thin polymer film on a heterogeneous substrate show a much difference manner and final structure from that on a homogenous substrate.

To start with, it is necessary to clarify the distinction among stable, metastable, and unstable films. This is straightforward in terms of the effective interface potential, φ(h), which is defined as the excess free energy per unit area necessary to bring two interfaces(solid-liquid and liquid-gas interface) from infinity to a certain distance h. The distance h is the initial thickness of the

liquid film. As shown in Figure 5, $h \to \infty$ induces $\varphi(h) \to 0$ indicating stability of a film with infinite film thickness.

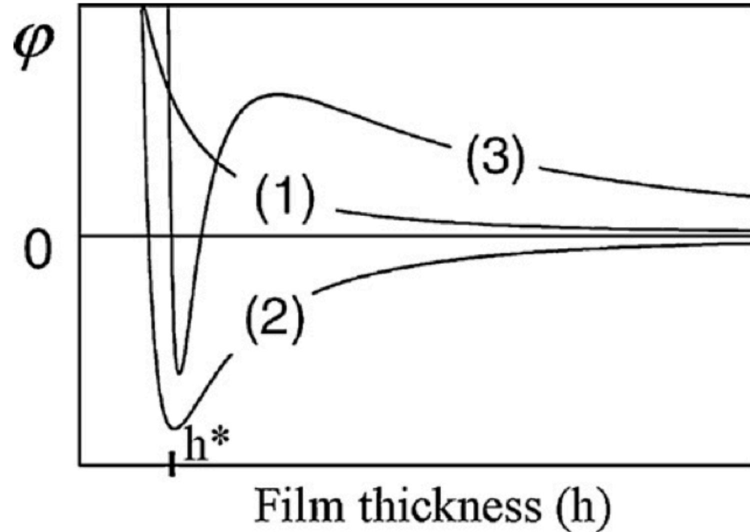

Figure 5. Effective interface potential φ(h) as a function of film thickness h for stable (1), unstable (2), and metastable (3) films. [11]

Curve (1) describes a scenario where $\varphi(h) > 0$ and where the global minimum lies at infinite film thickness. In this case the liquid film is stable. In curve (2), If the second derivative of φ with respect to film thickness is negative, $\varphi''(h_0)<0$, where h_0 is the initial thickness of thickness of the homogeneous film, the system is unstable, such that capillary waves on the film surface are spontaneously amplified under thermal annealing. The rupture mechanism is termed "spinodal dewetting"(fig. 6(a)). Such unstable modes exist whose amplitudes grow exponentially according to $\exp(t/\tau)$, where τ is the growth time that is characteristic for the respective mode. Furthermore, there is a characteristic wavelength λ_S of these modes the amplitude of which grows fastest and will therefore dominate the emerging dewetting pattern. In curve (3), the film is unstable for small film thickness, where $\varphi''(h)<0$, whereas for lager film thickness ($\varphi''(h)>0$), the film is

metastable. In the metastable case, the system has to overcome a potential barrier in order to reach its state if lowest energy at h=h*. Some kind of nuclei, e.g. dust particles or defects, are required to lower φ(h) and can therefore induce rupture of the film, a mechanism called “heterogeneous nucleation”. It is difficult to distinguish metastable and unstable mechanisms experimentally since both nucleation and spinodal dewetting can lead to dewetting in unstable films. Colse to the sign reversal of, thermal activation is sufficient to overcome the potential barrier for the nucleation of holes, a process called “ thermal nucleation” or “homogeneous nucleation” representing a third dewetting mechanism. The characteristic feature of homogeneous nucleation is a continuous breakup of holes (fig. 6(b)), whereas heterogeneous nucleation causes holes that emerge only within a narrow time interval (fig. 6(c)). Thus, the hole opening is most likely to happen at location having the smallest thickness, which can be caused by fluctuations of the film thickness or elevated region on the substrate.[11, 13, 14]

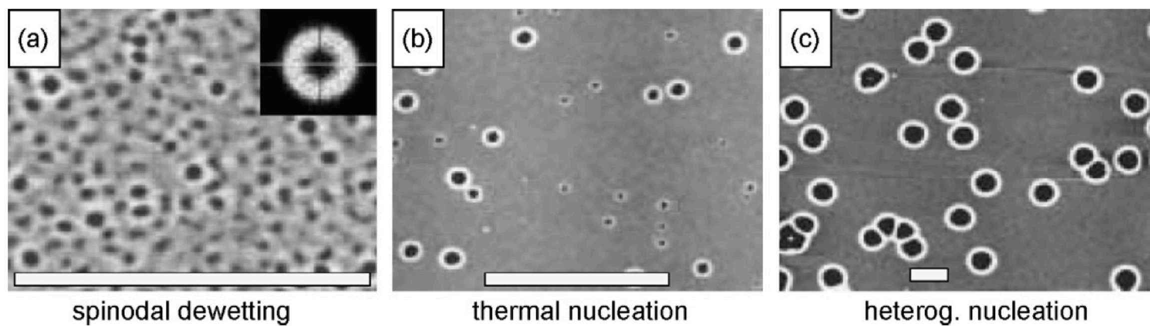

Figure 6. (a–c) AFM images of dewetting PS (2k) films. Scale bars indicate 5 μm, z-scale ranges from 0 nm (black) to 20 nm (white): (a) spinodal dewetting of 3.9 nm PS on type C wafer. The inset shows a Fourier transform of the image. (b) Thermal nucleation dewetting of 4.1 nm PS on type B wafer. (c) Heterogeneous nucleation dewetting of 6.6 nm PS on a type B wafer.[11]

1.3 Influence of native dioxide layer on the dewetting of polymer thin films

Thickness dependent interfacial potential were used to describe the stability of thin polymer films. Silicon wafers with their natural amorphous Si dioxide layer (SiO_x) have been widely used as the substrate. Thickness of the amorphous SiO_x layer plays a key role on the dewetting of polymer thin films. The figure 7 shows the relationship between polystyrene film thickness and effective interface potential Φ. In Figure 7, the dotted line represents the van der Waals potential, $\varphi(h)_{vdW}$, as given by Equation:

$$\varphi(h)_{vdW} = - A / (12\pi h^2) \qquad (4)$$

for a polystyrene film on a Si wafer, where A_{Si} is negative. The potential therefore is positive, purely repulsive and the PS film will be stable. However, $\varphi(h)_{vdW}$ for PS on an infinitely thick SiOx layer (solid line) is always negative, purely attractive and the PS film will be unstable, since the Hamaker constant A_{SiOx} is positive.

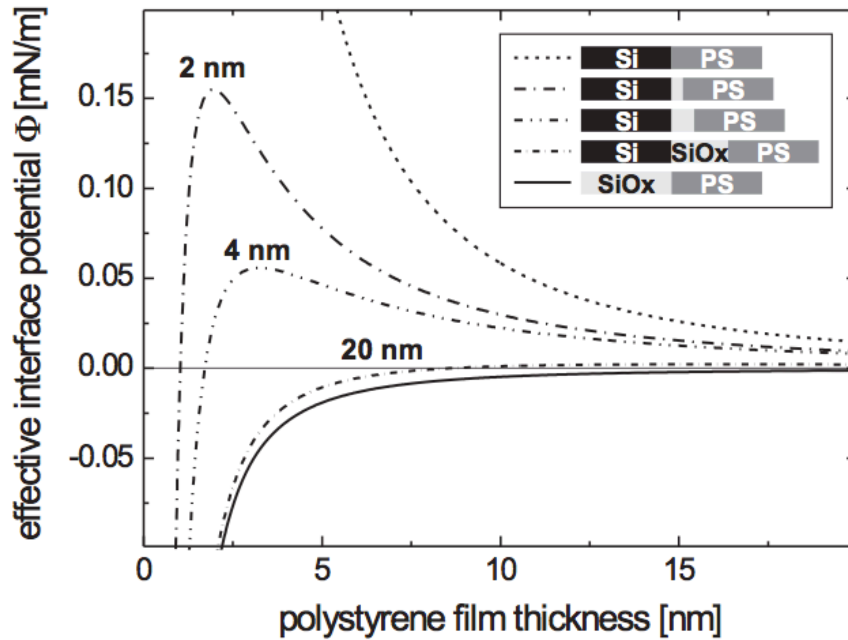

Figure 7. Long-range part of the effective interface potential φ(h) as function of PS film thickness h for different SiO_x layer thickness ranging from 0 nm (dotted line) to infinity (solid line), calculated with the formula given in Eq. (10). The Hamaker constants were calculated from the optical constants of the involved materials.[12]

Due to the $1/h^2$ dependence of the potential, the van der Waals forces are long-range forces and act significantly on distances up to about 100 nm. In stratified systems with more than one layer between the two half spaces of media 1 and 2, all mutual interactions have to be considered. A system like a PS film in air, spun on a thin silicon oxide layer on top of a Si wafer involves two thin layers (three interfaces, abbreviated as air/PS/SiOx/Si) and can be described by two Hamaker constants. Assuming additivity of forces, the system air/PS/SiOx/Si can be characterized by a summation of the van der Waals contributions of each of the single layers with thickness h of the PS and d_{SiOx} of the SiOx layer:

$$\phi_{vdW}(h) = -A_{SiO_x}/(12\pi h^2) + (A_{SiOx} - A_{Si})/12\pi(h + d_{SiOx})^2 \tag{5}$$

where A_{SiOx} and A_{Si} are the Hamaker constants of the respective system air/PS/SiOx and air/PS/Si. If the SiOx layer thickness is known, the Hamaker constants are calculated as shown before. Fig. 7 depicts the van der Waals potential as gained from Eq. (5). Clearly, the potential is influenced by the thickness of the silicon dioxide layer.[12, 15]

A stability diagram for the system air/PS/SiOx/Si is shown in Figure 8. The solid lines of the diagram separate the spinodal dewetting (unstable regime), where $\varphi''(h) < 0$, from in the regime of heterogeneous nucleation, characterized by $\varphi''(h) > 0$ (metastable regime). Thermal nucleation is possible for $\varphi''(h) = 0$, this line separates the two regimes. Experiments that exhibit spinodal

dewetting patterns are indicated by open symbols, those of heterogeneous nucleation (randomly distributed holes) are indicated by solid symbols. A star marks the set of parameters where thermal nucleation was observed. Note that in the unstable regime, heterogeneous nucleation from localized defects is also possible and indeed is sometimes observed.[11, 12]

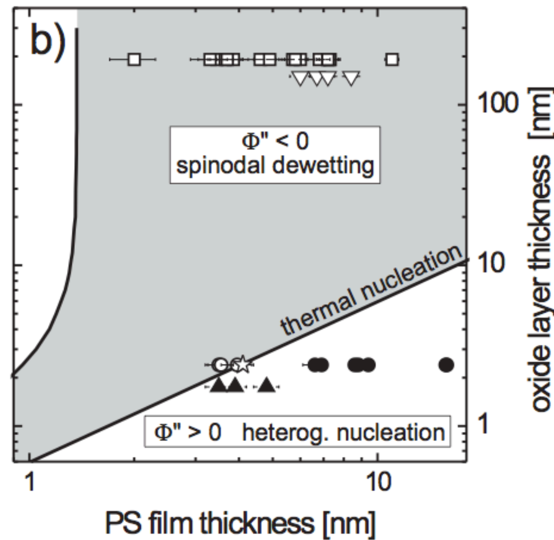

Figure 8. Stability diagram of PS films on top of Si wafers with variable oxide layer thickness.[12]

In this thesis, two types of silicon substrates were used: (1) native oxide silicon substrates (SiOx/Si), and the thickness of SiOx is 2.4nm; (2) hydrogen passivated silicon substrates (H-Si), and the thickness of SiOx is 1.3nm. The thickness of polystyrene films on these two types of silicon substrates is from 5nm to 100nm. According to the figure 8, the air/PS/SiOx/Si system in this study were metastable, and dewetting driving by the heterogeneous nucleation is expected in most of the cases (expect for 5 nm-thick films).

1.4 Adsorption of polystyrene at polymer/substrate interface

Several recent studies have shown that such non-equilibration nature is related to the

irreversible adsorption of polymer segments to the solid substrates [16, 17]. The formation of the adsorbed layer on solids, which can happen even when the polymer-substrate interaction is weak,[16] has a strong influence in the physical and mechanical properties of thin polymer films confined between the free surface and solid interface.[18-26] Recent studies have shown that PS chains are irreversibly adsorbed onto hydrogen-passivated silicon (H-Si) substrates from melts by annealing at a temperature much greater than T_g and that the adsorbed chains cannot be removed even after extensive rinsing with a good solvent for PS.[27] As shown in Figure 9, they reported that the thickness of the irreversibly adsorbed layer increases with increasing annealing time until it reaches equilibrium. More importantly, they demonstrated that such adsorbed layers are formed even on very weakly attractive substrate surfaces, that is, bare Si substrates, although the adsorbed layer thickness is much thinner than that for the PS/H-Si systems.

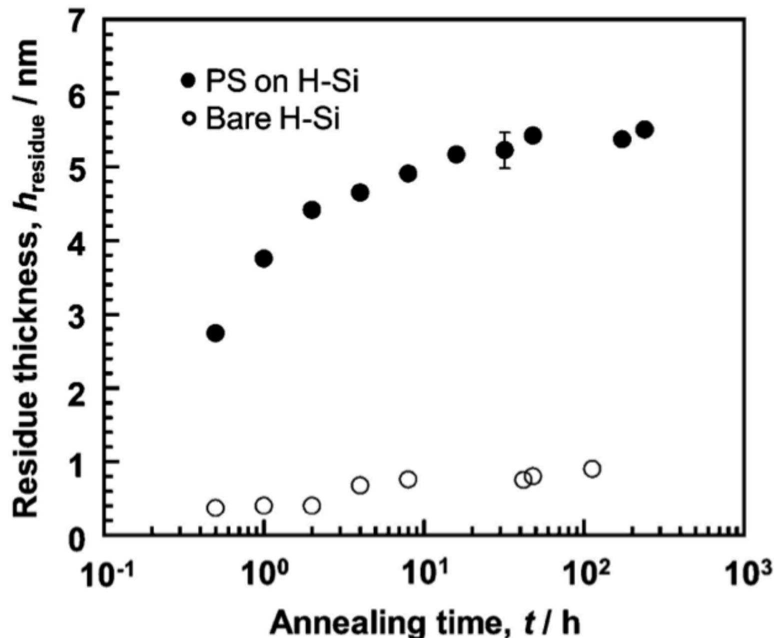

Figure 9. Annealing time dependence of the thickness of the residual film, $h_{residue}$, obtained for PS (M_w 1⁄4 44.1 kDa)/H-Si (solid symbols) and bare H-Si (open symbols). The

annealing was performed at T1⁄41501C in air. Figure reproduced from Fujii et al.[67] with permission from the American Chemical Society.[27]

At first glance, it seems that the adsorption of polymer chains and the dewetting of thin polymer filmsare two contradictory behaviors. Hence, the relationship between irreversible chain adsorption and the dewetting behavior needs to be clarified. Besides, studies need to be focused on the detail polymer structure at the solid interface in order to improve our understanding of wetting or dewetting of thin polymer films on solid substrate. Recent studies have shown that through physical adsorption, the flexible polymer chains, i.e. polystyrene adopt two different conformations on the solid surfaces due to piecemeal deposition[20, 22, 28-30]: the early arrived chains adopt a flattened conformation with chain parallel to the surface and form a compact, higher density layer relative to the bulk in equilibrium, while the later arrived chains are loosely adsorbed to the still-unoccupied empty cites by forming loops, as shown in figure 10 (the color line). Figure 10 also shows representative desorption kinetics for the adsorbed PS layer (Mw = kDa). Form the figure we can see that the thickness of the adsorbed layer decreases with increasing desorption time and reaches the final thickness of ~3.5nm after 120 days.

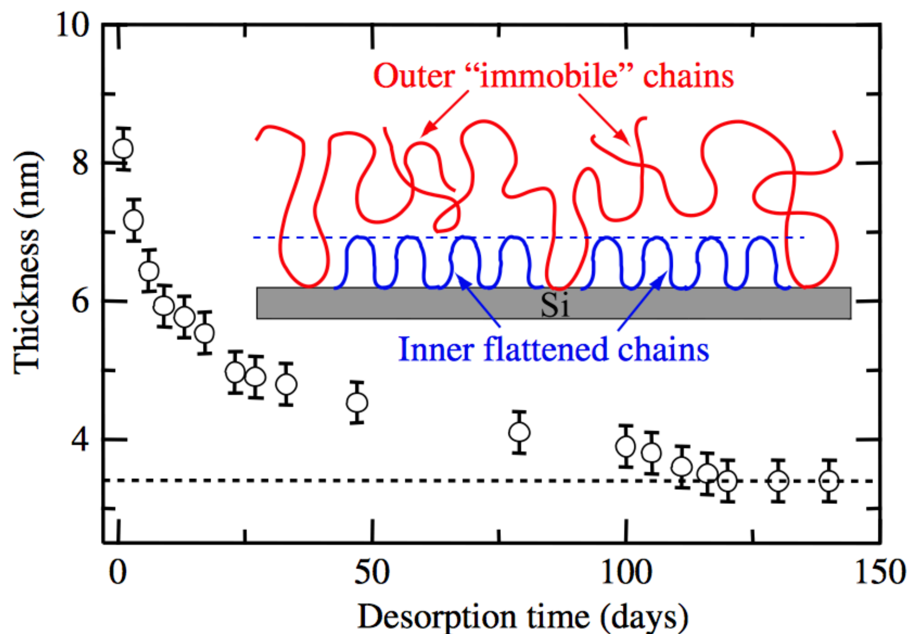

Figure 10. Desorption kinetics of the equilibrium adsorbed PS (Mw= 170 kDa) layer during the toluene leaching. The inset shows the schematic view of the two different chain conformations.[22]

Here, we show that the wetting/dewetting of thin polymer film on a solid substrate strongly depends on the detail nano-architecture of adsorbed chains at the polymer-solid interface. Low molecular PS film dewets on silicon substrate due to the absence of loosely adsorbed polymer chains at the substrate interface resulting from the limited chain length. However, the film could be stabilized if a loosely adsorbed PS layer is pre-deposited on the solid surface which provide "loops" structures for the free, low molecular weight PS chains to entangle or "hook" effectively.[20, 22, 27, 31] In contrast, the formation of flattened chains does not show a positive effect in stabilizing the film but may cause the film to rupture and dewet. The origin of wetting/dewetting behavior of thin PS films with different molecular weight on silicon substrate was explained based on the correlation between dewetting of thin PS films and the irreversible

adsorption of PS chains on solid surface.

1.5 Dewetting at a polymer-polymer interface

The more complex situation of a liquid dewetting from a liquid substrate has received much more attention in recent years. The liquid-liquid dewetting exhibit a variety of different regimes depending mainly on the relative viscosities of the two liquids, the thicknesses of the respective liquid layers, and the surface and interfacial tension involved.[32, 33] The solid surface can be programed from non-slippery (wettable) to slippery (nonwettable) by controlling the topmost surface chemically or structurally. For example, in the case of the polymer chains grafted to a solid, the repel chemically identical polymer molecules, depending on thegrafting density and the ratio of molecular weights of the non-grafted free chains to end-grafted polymer chains. This is the so-called "autophobic deweting" which is originated from the loss of configurational entropy of the grafted polymer chains. When the matrix polymers have the low grafting density, the free polymer chains penetrate to the grafted chains in order to maximize their translational entropy This will be the wetting region. However, when the matrix polymers have the high grafting density, the free polymer chains are expelled from the brush due to induce unfavorable stretching of free polymer chains. This will be the dewetting region.[34-36] Even though there has a large amount of dewetting studies, many issues are still unsolved: such as how the chain conformations affects the thin film wet or dewet from a substrate interface and what is the difference in mechanism between dewetting from a solid and autophobic dewetting from its own polymer layer.

Furthermore, it is also known that the thermal annealing process could facilitate the irreversible physisorption of polymer chains from the melt to the solid substrate, even when the polymer-substrate interaction is weak. By changing desorption energy such as different solvent, we can

create two different chain conformation in the direction normal to the surface: the flattened chains that constitute the inner higher density region and loosely adsorbed polymer chains that form the outer bulk-like density region. The inner flattened layer have many contact points and have high surface coverage.[21, 22, 31, 37, 38]These conformations of adsorbed chains at the solid-polymer interface should be considered as an important factor which causes the dewetting of the thin polymer films. It has also been found that the autophobicity maybe lost and wettability maybe reestablished by adding long polymers due to the pinning of the chains. These adsorbed chains can also act as "connectors" that cause a resistance force against the driving capillary forces for dewetting.[10, 21] In this thesis, monodisperse polystyrene (PS) with different molecular weights were used to study the dewetting behavior on silicon substrates. Low molecular weight polystyrene (PS) thin film dewet on both the native silicon oxide (SiO_X/Si) and hydrogen passivated silicon (H-Si) substrate via autophobic dewetting: a 2 nm-thick flattened interfacial PS nanolayer wets the solid substrate upon annealing while the rest of the same PS molecules is not further wetted by such flattened nanolayer leading to the formation of droplets. However, the dewetting can be effectively prevented by forming a loosely attached interfacial sublayer at the substrate interface. As we will show, the detail architecture of adsorbed chains plays a key role in determine the stability of polystyrene films.

Chapter 2 Experimental Section

2.1 Sample Preparation

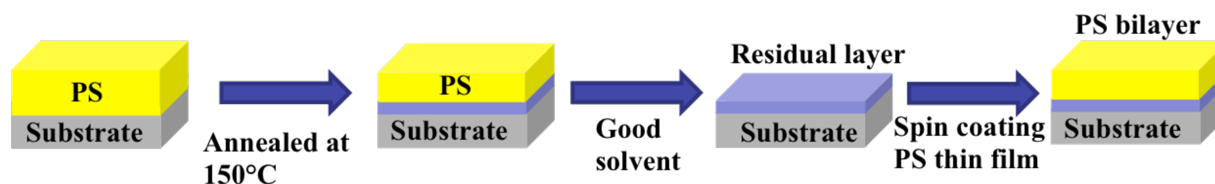

Scheme 1. Sample preparation process used in experiment

Monodisperse polystyrene (PS) with eight different molecular weights (M_W = 3.7 kDa, 13.1 kDa, 30kDa, 50 kDa, 123 kDa, 170 kDa, 290 kDa and 650 kDa, M_W/M_n < 1.2, Scientific Polymer Products Inc. or Pressure Chemical CO.) were used to study the dewetting behavior on silicon substrates. The bulk glass transition temperature (T_g) of PS was determined to be T_g = 100 °C by differential scanning calorimetry. Native oxide silicon wafers (hereafter denoted as SiO_x/Si substrates) were cleaned by immersion in a hot piranha solution (i.e., a mixture of H_2SO_4 and H_2O_2, *caution*: the *piranha solution* is highly *corrosive* upon contact with the skin or eyes and is an explosion hazard when mixed with organic chemicals/materials; Extreme care should be taken when handing it.) for 30 min, subsequently rinsed with deionized water thoroughly. By using x-ray reflectivity, we confirmed that the SiO_x layer after piranha solution cleaning is about 2.4 nm thick on the Si with a surface roughness less than 0.5 nm. The water contact angle of such SiO_X/Si substrate is estimated to be less than 5°, an indication of the hydrophilic nature of the surface. Hereafter, we assign the Si substrates cleaned with piranha solution as B-Si substrates. The cleaned native oxide silicon (SiO_x/Si) wafers (or B-Si substrates) were further cleaned by immersion in an aqueous solution of hydrogen fluoride (HF) for 30s to remove the native oxide (SiO_x) layer (hereafter denoted as H-Si substrates). However, as been reported previously[39], we

confirmed that a SiO_x layer of about 1.3 nm in thickness was reproduced after HF etching due to atmospheric oxygen and moisture. All the silicon cleaning were precisely controlled with the same procedure to avoid the possible difference in the chemistry of the oxide layer on the dewetting behavior of the spin coated PS films.[40] PS thin films with average thicknesses ranging from 5 nm to 100 nm were prepared by spin coating PS/toluene solutions onto both B-Si substrates and H-Si substrates with a rotation speed of 2500 rpm. The thicknesses of the spin-cast PS thin films were measured by an ellipsometer (Rudolf Auto EL-II) with a fixed refractive index of 1.589.

On the other hand, the PS flattened layer and interfacial sublayer on B-Si substrates or H-Si substrates were prepared by the established protocol reported previously[20]: First of all, PS thin films (~ 50 nm in thickness) were annealed at T = 150 °C for prolonged times (up to 150 h) in an oil-free vacuum oven (below 10^{-3} Torr). As reported previously, the "quasiequilibrium" flattened layer and interfacial sublayer[20] were formed by prolong annealing (several hours to days) at T = 150 °C, depending on the molecular weight of PS. The annealed films were then solvent leached in baths of chloroform for the flattened layer and toluene for the interfacial sublayer at room temperature, respectively. This selective extraction of the two different adsorbed nanolayers is possible due to the large difference in the desorption energy between the outer loosely adsorbed chains and the flattened chains, which is proportional to the number of segment-surface contact point[29]. The resultant interfacial sublayers and flattened layers were post-annealed at 150 °C under vacuum overnight to remove any excess solvent molecules trapped in the films. The scheme of sample preparation is shown in Scheme 1.

The polymer used was poly (2-vinylpyridine) (P2VP, M_W = 219 kDa, M_W/M_n < 1.11, Scientific Polymer Products Inc.). The bulk glass transition temperature (T_g) of P2VP was

determined to be T_g = 98 °C by differential scanning calorimetry. The P2VP flattened layer and interfacial sublayer on B-Si substrates were prepared by the established protocol reported previously[20]: Firstly, P2VP thin films (~ 20 nm in thickness) were spun cast from a dimethylformamide (DMF) solution onto Si substrates which were pretreated with a hot piranha solution (i.e., a mixture of H_2SO_4 and H_2O_2) for 30 min and subsequently rinsed with deionized water thoroughly; Secondly, Spin cast films were annealed at T = 190 °C for prolonged times (up to 200 h) in an oil-free vacuum oven (below 10^{-3} Torr). As reported previously, the "quasiequilibrium" flattened layer and interfacial sublayer[20] are formed after 100 h annealing under the isothermal condition. Finally, the films were solvent leached in baths of fresh DMF forthe flattened layer and cholorobenzene for the interfacial sublayer at room temperature, respectively. This selective extraction of the two different adsorbed nanolayers is possible due to the large difference in the desorption energy between the outer loosely adsorbed chains and the flattened chains, which is proportional to the number of segment-surface contacts[29]. The resultant interfacial sublayers and flattened layers were post-annealed at 190°C under vacuum overnight to remove any excess solvent molecules trapped in the films.

2.2 Atomic Force Microscope (AFM) measurements.

The surface morphology of the adsorbed layers and thin polymer films were studied by using atomic force microscope (AFM) (Digital Nanoscope III). The standard tapping mode was conducted in air using a cantilever with a spring constant of 40 N/m and a resonant frequency of 300 kHz. The scan rate was 1.0 Hz with the scanning density of 256 or 512 lines per frame.

2.3 Optical Microscope (OM) Measurements.

Optical microscope (OM) measurements were conducted by using reflective light under an Olympus BHT Microscope equipped with differential interference contrast attachment for

incident light after Nomarski (NIC Model). OM images were captured by a digital camera under polarized light at room temperature.

Chapter 3 Result and discussion

3.1 Molecular weight dependence of polystyrene films on silicon substrates.

Figure 11 (a-j) shows representative optical images for PS (Mw=3.68 kDa, 13.1 kDa, 30 kDa, 50 kDa, 123 kDa) 20nm-thick spin cast films on hydrogen passivated H-Si and SiOx-Si substrates after thermally annealed at 150 ºC for 9 days. Note that the thickness of SiOx layer for H-Si and SiOx-Si substrates was 1.3nm and 2.4nm, respectively. The PS thin films composed of Mw= 3.68 kDa, 13.1 kDa, 30 kDa and 50 kDa broke up into droplet-based cellular patterns on both two silicon substrate after the course of annealing, indicating that the polymer completely dewet from the substrate and aggregated into spherical droplets.[12] It should be note that the average distance between neighboring droplets is largely decreased with decreasing of film thickness, consistent with previous studies. However, with the same film thickness, it can be seen that spherical droplets for 30 kDa and 50 kDa PS film is apparently denser than those formed in 3.68 kDa, 13.1 kDa films, with much smaller distance between neighboring droplets. On the other hand, no sign of dewetting was observed for PS (M_w = 123 kDa) thin films on both substrates and the same is true for 20 nm-thick PS thin films composed of M_w larger than 123 kDa. To explore the structure of dewetted film at the microscopic scale, AFM measurements were performed by zoom-in to the dewetted regions. Figure 11 (k-r) shows the surface morphologies of the dewetted PS films (correspond to the samples shown in Figure 11 (a-d) and (f-i)) at the dewetted areas. For lower molecular PS (3.68 kDa and 13.1 kDa) films on both substrates, the dewetted region are homogeneous and featureless. However, microscopic structures are formed at the dewetted regions while the 30 kDa and 50 kDa films dewet completely from the substrates.

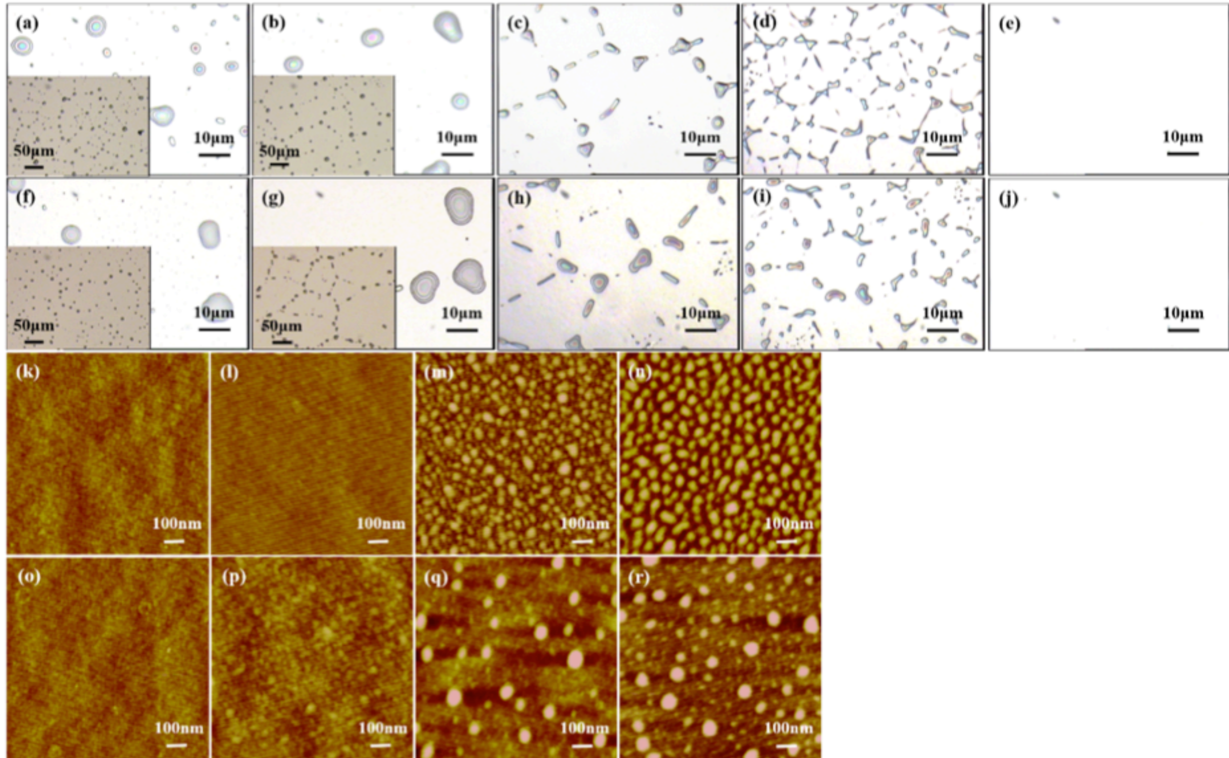

Figure 11. OM images of 20 nm-thick PS films with five different M_w, 3.68 kDa (a, f), 13.1 kDa (b, g), 30 kDa (c, h), 50 kDa (d, i) and 123 kDa (e, j) on bare H-Si (a-e) and SiO_x/Si (f-j) substrates after thermally annealed at 150 °C under vacuum for 9 days. The insets in (a), (b), (f) and (g) are the OM images with a smaller magnification of the same sample. The nanoscale surface morphologies (AFM images) of the dewetted regions in (a-d) and (f-i) were shown in (k-n) and (o-r), respectively. The height scale for the AFM images is 0 – 10 nm.

On H-Si substrate, dimple structures with the characteristic length of about several tenth of nanometers were formed at the dewetted regions. The average height of these "textures" from the SiO_x surface was estimated to be about 2-3 nm based on the cross sectional analysis of Figure 11 (m, n). As we will show later, these microscopic structures on H-Si substrate correspond to the

"flattened layer" in which the PS chains strongly adsorb on a H-Si substrate, resulting in a higher density monolayer relative to the bulk density.[20, 22] In contrast, large micelle-like structures with an average height of $2R_g$ (R_g is the unperturbed radius of polymer gyration) were formed at the dewetted region on SiO_x/Si substrate. At the same time, the large micelles were also surrounded with some small dimple structures. These results indicate that polymer chains are prefer to aggregate into random coils instead of flatly attached to the solid surface due to the relatively weaker interaction between the PS and SiO_x/Si substrate.

3.2 How molecular weight affect the formation of adsorbed layer near the substrates interface?

To clarify whether there is chain adsorption occur on the silicon substrate in both dewetting and wetting scenarios, we leached the dewetted film with solvents at room temperature. According to previous study[20], the desorption energy can be easily adjusted by tuning the leaching conditions which enable us to distinguish the formation of loosely adsorbed chains and flattened chains independently. Here, we used the same leaching conditions applied previously[20]. One is the toluene-leaching process which allow us to remove the unadsorbed chains but loosely adsorbed chains are able to survive from this mild leaching condition. Another is the stronger chloroform-leaching process which allow us to remove both unadsorbed chains and loosely adsorbed chains, and only flattened chains are stable against this leaching process. Figure 12 shows the resultant thickness of the PS films after two different leaching process as a function of M_w (ranging from 3.68 kDa to 650 kDa). It can be seen that when $M_w \geqslant 123$ kDa, different leaching conditions result in very different residual layers. For toluene leaching process, the thickness of the residual layer follows the relationships of $h_{ad} = 0.65\ R_g$ and $h_{ad} = 0.46\ R_g$ ($R_g = \sqrt{Mw/(104{\times}6)}{\times}a$,

where a is the segment length of PS) for H-Si substrate and SiO_x/Si substrate, respectively, which are in good agreement with previous results[22, 37].

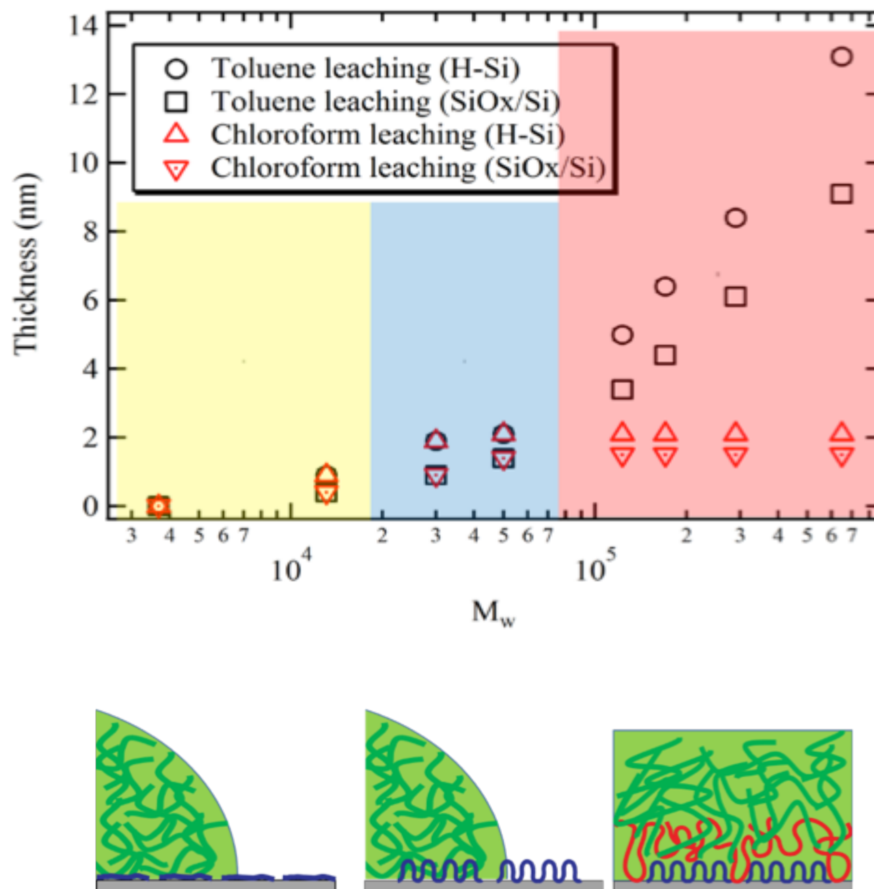

Figure 12. Thicknesses of the residual PS layers on H-Si and SiO_x/Si substrates as a function of M_w after leaching with toluene (lower desorption energy) or chloroform (higher desorption energy). The original PS films (20 nm-thick) were thermally annealed at 150 °C under vacuum for 9 days before the leaching process.

And from the AFM height images of the 123 kDa PS residual layers, as shown in Figure 13 (e) and (k), we can see that the residual layers are flat and featureless on both substrate and similar homogeneous residual layers were also found for all the higher M_w ($M_w \geqslant$ 123 kDa) PS films after the toluene leaching. These results indicate that loosely adsorbed layers are formed when

$M_w \geqslant 123$ kDa. At the same time, if we apply the chloroform-leaching process, the thickness of the residual layer no longer displays M_w dependence and the surface is no longer homogeneous on both substrate, indicate the residual layers after the chloroform leaching correspond to the high density flattened layer. On the basis of previous studies[20], the apparent dimple structure shown in Figure 13 (f) and (l) is likely due to the low effective grafting density which results from the relatively weak interaction between PS and H-Si or SiO_x/Si substrate.

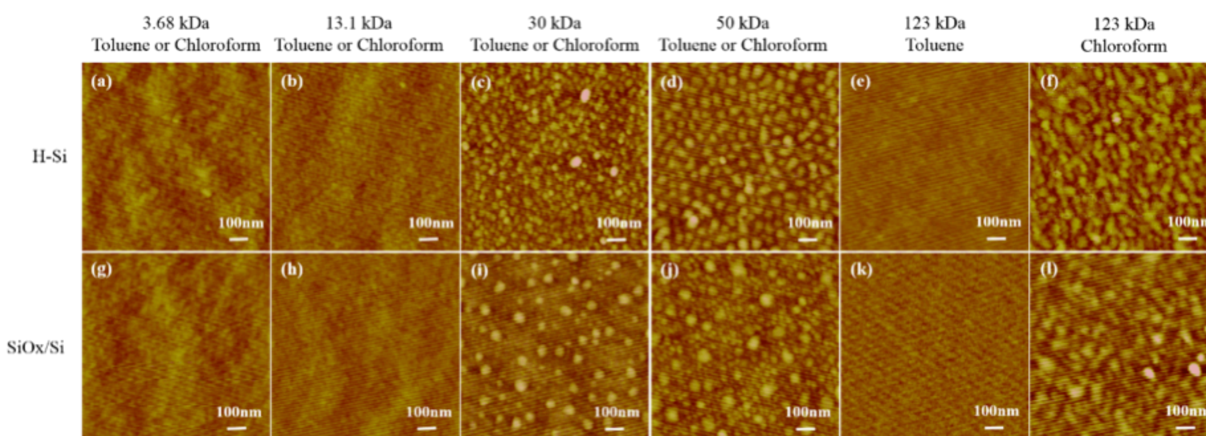

Figure 13. The surface morphologies of the residual PS layers on H-Si and SiO_x/Si substrates as a function of M_w after leaching with toluene (lower desorption energy) and/or chloroform (higher desorption energy). The original PS films (20 nm-thick) were thermally annealed at 150 °C under vacuum for 9 days before the leaching process. The height scale for the AFM images is 0 – 10 nm.

On the other hand, when $M_w \leqslant 50$ kDa, the two leaching process no longer shows a significant deference in the thickness as well as the surface morphology of the residual layer. If the difference in the desorption energy between toluene and chloroform also applies for low M_w PS, these results indicate that no loosely adsorbed layer are formed when $M_w \leqslant 50$ kDa. This is possibly due to the short of chain length which makes the polymers difficult to build "bridges"

(loops) among the available empty spaces. In other word, only flattened layers were formed when $M_w \leqslant 50$ kDa. Nevertheless, as shown in Figure 12 and Figure 13 (a-d) (g-j), there is an obvious different in the surface feature and the thickness of the PS residual layer between higher M_w (30 kDa and 50 kDa) and low M_w (3.68 kDa and 13.1 kDa). For 30 kDa and 50 kDa PS, the residual layer are almost the same in thickness and similar surface structures as the one formed in 123 kDa or higher M_w PS films, although the thickness of the 30 kDa residual layer is slightly thinner. However, for 3.68, 13.1 kDa PS, the residual layers are almost featureless at the surface and become much thinner in thickness. X-ray photoelectron spectroscopy (XPS) measurements further evident that there are still polystyrene remained on the silicon substrate even the thickness of the residual layer is almost undetectable.

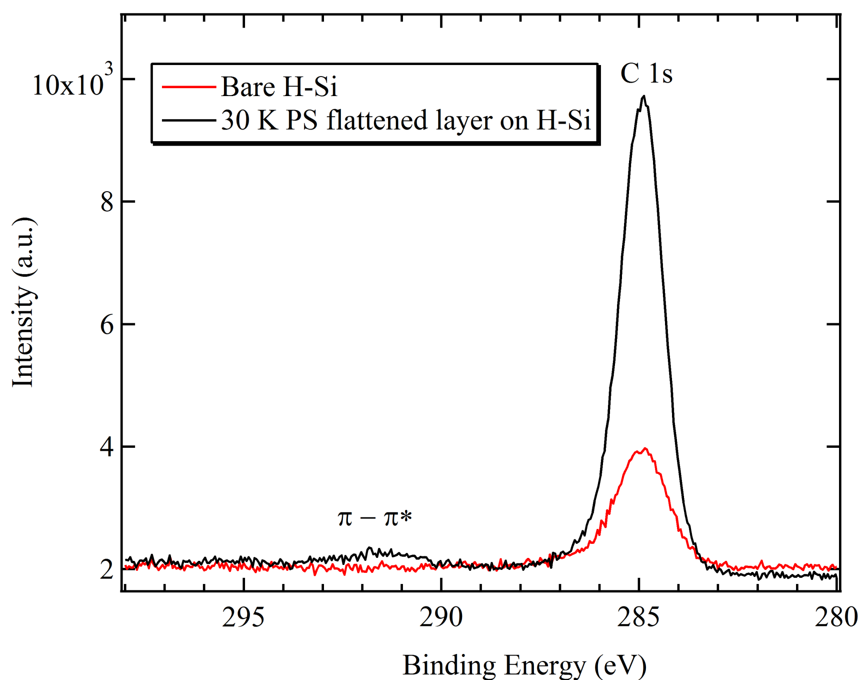

Figure 14. X-ray photoelectron spectroscopic C 1s narrow scan of the residual film obtained from 30 kDa PS flattened layer on H-Si after annealing at 150 ºC for 9 days followed by thorough rinsing in chloroform.

Figure 14 shows the XPS spectrum of a residual film obtained from 30 kDa PS flattened layer on H-Si after annealing at 150 ºC for 9 days followed by thorough rinsing in chloroform. The prominent peak seen in the spectrum, with a binding energy of 285.0 eV, is identifiable with the C 1s peak typically found in hydrocarbons. The shakeup peak, corresponding to the π-π* transition of the phenyl group with a binding energy between 291.0 and 293.0V is also clearly discernible.[37] These results indicate that the M_w independent flattened layer, as reported previously, does not valid any more when Mw ≤ 13.1 kDa.

3.3 Correlation between chain adsorption and the dewetting of polystyrene films.

Comparing with Figure 11 (k-r), it can be seen that the overall surface morphologies of the PS residue layers ($M_w \leqslant 50$ kDa) (Figure 13 (a-d) (g-j)) are very similar to those of the structure at the dewetted regions in the original thin films. However, there are some changes during the solvent-leaching process. For 30 kDa and 50 kDa PS on H-Si substrate (Figure 13 (c) and (d)), a slight decrease in the average height of the dimple structures is observed after the solvent leaching, while the average diameter of the dimple structures become larger. If the mass is conserved before and after the leaching process, the collapse of the dimple structures indicates that polymer chains become more flatly attached to the substrate in order to maximize the surface-segmental contacts. Such behavior may because of the presence of solvent enhances the segmental mobility of flattened chains near the interface and facilitates the flattened chains to achieve a conformation more close to equilibrium (adsorbed more effectively) than the one formed via thermal annealing. For 30 kDa and 50 kDa PS on SiO_x/Si substrate (Figure 13 (i) and (j)), the average height of large micelles decrease from $2R_g$ to less than $1R_g$ after solvent leaching without a significant change in the diameter of the micelles. Considering the relatively weak interaction between PS and SiO_x/Si substrate, it is reasonable that some polymers within

the original micelles in Figure 11 (q) and (r) are not well adsorbed to the substrate hence are removed during the solvent leaching process. But still, based on the overall surface morphology before and after solvent leaching, it is clear that when the 30 kDa and 50k Da PS 20 nm-thick films dewetted into macroscopic droplets on silicon substrate, there is a very thin flattened layer remained at the polymer-substrate interface. Similar results were also found for the thermal equilibrium 5 nm-thick dewetting PS films (M_w = 30 and 50 kDa), although the kinetics become very different (faster when film become thinner). From the AFM result, we also found that the flattened layer is already formed while the film is still at the early stage of dewetting, as shown in figure 15. This is not surprising since the formation of the PS flattened layer only takes few hours or even less[20]. Hence, the dewetting of 30 kDa and 50 kDa PS films is not happening on a "bare" silicon surface, developing in the presence of a thin flattened layer.

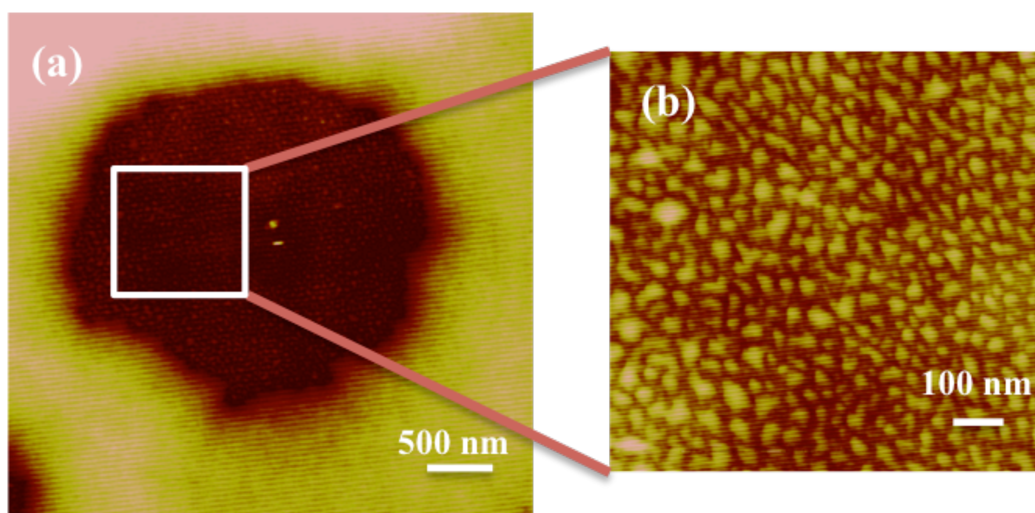

Figure 15. (a) show AFM images of 5 nm-thick PS 30K films on H-Si substrate. The original PS films were thermally annealed at 150ºC under vacuum for 9 days. The surface morphologies of the dewetted region in (a) were shown in (b). The height scale for the AFM images is 0-10nm.

It is known that when the PS films with fixed film thickness are prepared on the same substrate, the effective interfacial potentials are expected to be the same regardless of the choice of molecular weight. However, a clear M_w dependence is observed from Figure 11. In fact, the film stability and chain adsorption of the 20 nm-thick spin cast PS films prepared on two different silicon substrate can be divided into three categories depending on their molecular weight, as highlighted in Figure 12. For lower molecular weight (M_w = 3.68 kDa and 13.1 kDa), there is almost no chain adsorption at the polymer-substrate interface and the films dewet on both substrate with a large distance between the nearest droplets. For intermediate molecular weight (M_w = 30 kDa and 50 kDa), the films also dewet on both substrate but the distance between the nearest droplets become much smaller. At the same time, there is a flattened layer already formed at the polymer-substrate interface during the early dewetting process. For higher molecular weight ($M_w \geqslant$ 123 kDa), both flattened layers and loosely adsorbed layers are formed at the polymer-substrate interface and the film remained stable even after long time annealing. Hence, a correlation between the film stability and the formation of adsorbed layer at the polymer-substrate interface is clearly observed.

3.4 The role of the flattened layer and loosely adsorbed layer.

In order to unveil the correlation between the film stability and interfacial structures, we modified the silicon substrate by pre-depositing a PS flattened layer (50 kDa or 650 kDa) (h_{fl} = 2.1 nm on H-Si and h_{fl} = 1.5 nm on SiO_x/Si) or loosely adsorbed layer (123 kDa or 650 kDa) (h_{ad} ~ 0.65Rg on H-Si and h_{ad} ~ 0.46Rg on SiO_x/Si) before we spin cast the PS films. Figure 16 shows the OM images of 20 nm-thick PS films ($M_w \leq$ 123 kDa) prepared on the flattened layer-modified or loosely adsorbed layer-modified silicon substrate after annealed at 150 ºC for more than 9 days. Since both flattened layer and loosely adsorbed layer are stable against toluene, the

PS overlayers were directly spin-coated onto these modified substrate from the toluene solution. As seen, the 20 nm-thick PS overlayer with $M_w \leq 50$ kDa completely dewet on the PS 650 kDa flattened layer modified H-Si substrate. In contrast, no dewetting were observed when the M_w of the top 20 nm-thick PS overlayer is 123 kDa or larger. Similar results were also observed when PS 50 kDa flattened layer or SiO_x/Si substrate was used.

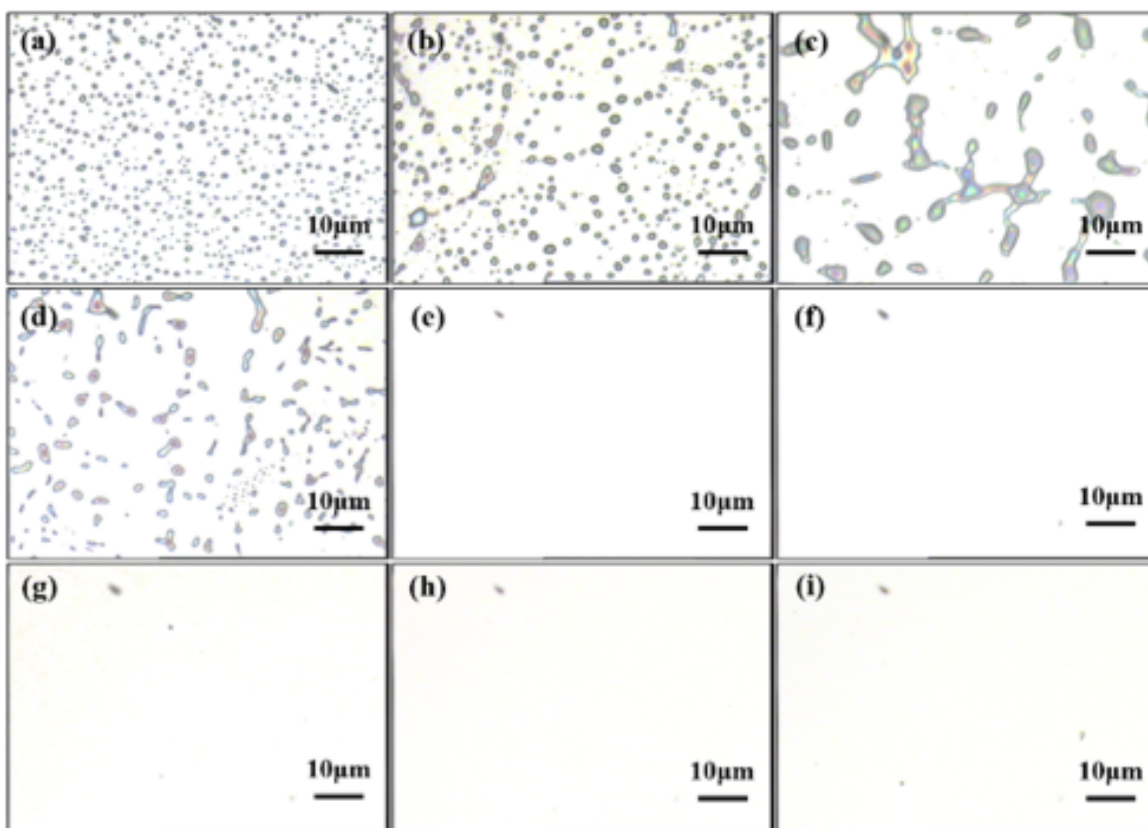

Figure 16. (a-e) shows OM images of 20 nm-thick PS films with five different M_w, 3.68 kDa (a), 13.1 kDa (b), 30 kDa (c), 50 kDa (d) and 123 kDa (e) on PS flattened layer (M_w = 650 kDa) modified H-Si substrate after thermally annealed at 150 °C under vacuum for 9 days. (f-i) shows OM images of 20 nm-thick PS films with two different M_w, 3.68 kDa (f, g) and 50 kDa (h, i) on PS loosely adsorbed layer (M_w = 650 kDa) modified H-Si (f, h) and SiO_x/Si (g, i) substrates after thermally annealed at 150 °C under vacuum for 9 days.

After leaching the bilayers with toluene, an increase in the residual thickness (compared to the original thickness of flattened layer) was found only when $M_w \geq 123$ kDa, as shown in figure 17, indicating long polymer chains within the overlayer "reel-in" the empty spaces of flattened layers (~ 30% of the entire film surface) and further developing the formation of the loosely adsorbed chains that form bridges jointing up nearby empty sites. However, the no loosely adsorbed layer was reformed when $M_w \leq 50$ kDa, possibly due to the short of chain length which makes the free chains difficult to pin from one empty site to another.

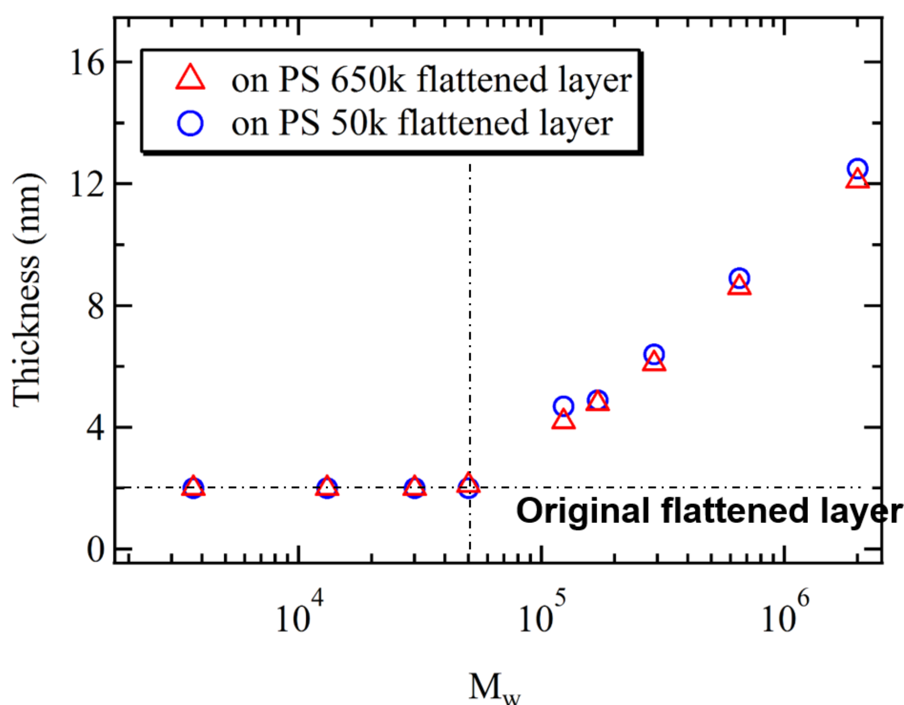

Figure 17. The thicknesses of the residual PS layers on 650K or 50K flattened layer as a function of M_w after leaching with toluene. The original bilayers were thermally annealed at 150 °C under vacuum for 9 days before the leaching process.

On the other hand, when the 20 nm-thick PS overlayers ($M_w \leq 123$ kDa) were prepared on PS 650 kDa loosely adsorbed layer-modified silicon substrate, no sign of dewetting was observed

under both OM and AFM even after thermally annealed at both 150 ºC and 190 ºC for more than 9 days. These results indicate that the two different nano-architectures of adsorbed chains at polymer-solid interface play a key role in the wettability of PS films on silicon substrate: the M_w dependent loosely adsorbed chains facilitate the top film to stabilize against dewetting, while the flattened chains does not help in the stabilization of the top film but as we will show later, may cause dewetting of the top film instead.

Comparing Figure 11 (a-b) and Figure 16 (a-b), it can be seen that the average minimum distance between neighboring droplets were largely decreased when the 20 nm-thick 3.68 kDa and 13.1 kDa PS films dewetted on the flattened chains-modified H-Si substrates. Such difference was also observed when SiO_x/Si substrate was used. In contrast, no significant difference were observed in case of 30 kDa and 50 kDa PS films on bare silicon substrates Figure 11 (c-d) and flattened chains-modified substrates Figure 16 (c-d). This is not surprise since the flattened layers were also formed 30 kDa and 50 kDa PS single films formed on the bare silicon substrate during thermal annealing and we know that the flattened layer is almost independent of M_w when $M_w \geqslant 30$ kDa. However, for the single 3.68 kDa and 13.1 kDa PS films prepared on bare silicon substrate, there is almost no flattened chains formed at the polymer-substrate interface. Hence, the polymeric materials were flow in the presence of bare silicon surface during the dewetting process. However, in the presence of flattened layer, flow rates may increase during the dewetting of PS films due to the relative high friction between polymer materials and the flattened chains, leading to a significant decrease in the average minimum distance between neighboring droplets.

To understand the underlying mechanism that causes the opposite wettability of flattened chains and loosely adsorbed chains on thin PS films, we used the both the static and dynamic contact

angle measurements and elucidated that the static water contact angles for the 2 nm-thick PS flattened layer and the M_w dependent PS loosely adsorbed layer are identical to that of a 50 nm-thick spin cast PS film, while the dynamic contact angle measurements show a nearly 10º larger in the hysteresis for the flattened layer, possibly due to the surface heterogeneity caused by the presence of dimple structures, as shown in figure 18.

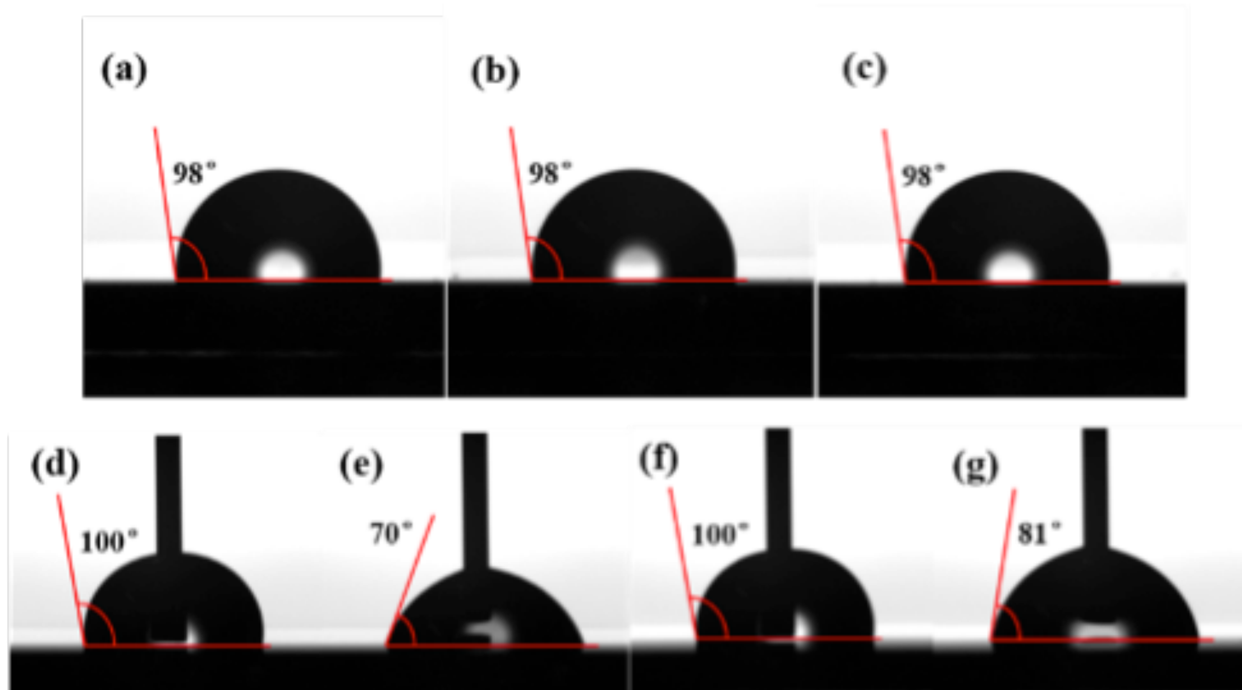

Figure 18. The representative static water contact angles of (a) 123kPS flattened layer, (c) 123kPS interfacial sublayer, (d) 20nm-thick 123kPS spin cast film. The representative dynamic water contact angles of 123kPS flattened layer during the advancing and receding process were shown in (d) and (e), respectively. The representative dynamic water contact angles of 123kPS interfacial sublayer during the advancing and receding process were shown in (f) and (g), respectively.

Considering the large heterogeneity of PS flattened layer, we alternatively used poly (2-vinylpyridine) (P2VP, M_w = 219 kDa, M_w/M_n = 1.11, Polysciences Inc.) which enables us to prepare homogenous flattened layers on SiO_x/Si substrates due to the more favorable polymer-substrate interactions [20]. The bottom P2VP flattened layers (~ 3 nm in thickness) or loosely adsorbed layers (~ 8 nm in thickness) were first prepared on the SiO_x/Si substrate and the 20 nm-thick PS were prepared on these modified substrates by directly spin-coating of a toluene solution. After thermally annealed at T=150 °C under vacuum for long time (more than 7 days), it was found the 20 nm-thick PS films completely dewet on the P2VP flattened layer-modified substrates, as shown in figure 19 (a-d). As seen, the 20 nm-thick PS overlayer with lower molecular PS (3.68kDa and 13.1kDa) completely dewet on the P2VP 219kDa loosely adsorbed layer-modified substrates, as shown in figure 19 (e-f), as the length of the free chains is too short to entangle with the outer loosely adsorbed polymer chains. In contrast, no dewetting were observed when the M_w of the top 20 nm-thick PS overlayer is 30 kDa or larger, as shown in figure 19 (g-h). This results again evident that the hindrance of the dewetting is correlated with the formation of the loosely adsorbed chains at the polymer-solid interface. All these results again reveal that the two different adsorbed chain nano-architectures play opposite roles in controlling the stability of polymer thin films. At the same time, we found that both static and dynamic water contact angle measurements for the P2VP flattened layer and loosely adsorbed layer are identical to that of a thick (50 nm-thick) P2VP spin cast film, indicate that the difference in the wettability of the flattened layer is related to the change in the interfacial tension (not an enthalpic contribution).

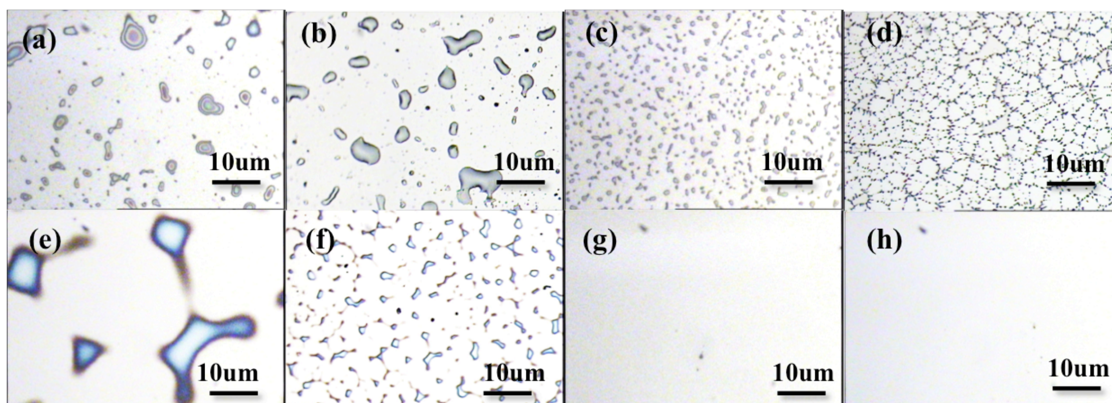

Figure 19. (a-d) shows OM images of 20 nm-thick PS films with four different M_w, 3.68 kDa (a), 13.1 kDa (b), 30 kDa (c), 50 kDa (d) on P2VP flattened layer (M_w = 219 kDa) modified SiO_x-Si substrate after thermally annealed at 150 ºC under vacuum for 7 days. (e-h) shows OM images of 20 nm-thick PS films with four different M_w, 3.68 kDa (e), 13.1 kDa (f), 30 kDa (g), 50 kDa (h) on P2VP loosely adsorbed layer (M_w = 219 kDa) modified SiO_x-Si substrates after thermally annealed at 150 ºC under vacuum for 7 days.

Hence, we postulate that the loosely adsorbed chains act as connector molecules, in analogue to the autophobicity of end-grafted polymers.[10, 41] It should be emphasized that the chain conformation of the connector is polymer loops. As noted previously[42, 43], polymer loops at the interface can efficiently entangle with free polymer chains when the grafting density is small enough, while resulting in favorable adhesion properties. It is known that irreversibly adsorbed polymer chains form three types of segment sequences, “trains” (adsorbed segments), “loops” (sequences of free segments connecting successive trains), and “tails” (non-adsorbed chain ends)[44]. According to previous computational results on chain conformations of adsorbed chains at the polymer melt/solid interface[44], the average number of segments belonging to loops

increases (up to ~ 30 %) with increasing N (up to N = 10,000), while that belonging to tails is more dominant (~ 65%). Dadmun and co-workers reported that such loop conformation at the interface plays an important role in improving the interfacial adhesion between different phases.[45, 46] Hence, it this reasonable to deduce that the formation of the loops in the loosely adsorbed polymer layers provide structures to which free or unbound polymer chains can entangle, effectively improving the film stability at the solid-polymer melt interfaces.

On the other hand, the flattened chains fail to stabilize the film possibly due to two major reasons. One possibility is the excess entropy loss caused by the unfavorable stretching of molecules when the free polymer melt is in contact with the flattened layer, analogue to the autophobic behavior", in which conformational entropic loss that occurs when free polymer chains penetrate into end grafted polymer chains due to the unfavorable stretching[34, 47-49] plays a crucial role. Based on X-ray reflectivity analysis, we have found PS and P2VP flattened layers has a relative higher density (about 10%) compare to their bulk values. Hence, penetration of unadsorbed chains into the denser flattened layer is unfavorable and may cause destabilization of the polymer-flattened layer interface. Another major reason we believe is the many surface-segmental contacts of flattened chains which may exacerbate the entanglements with unadsorbed chains, since the tube diameter here will be determined by the distance between adsorption sites which is smaller relative to those for the bulk. According to previous studies, we can approximate that the loop size of the flattened chains correspond to R_g^{loop} where R_g^{loop} is the radius of polymer gyration of the loop[22]. Based on the critical molecular weight for entanglement (N_e=173 for PS and P2VP)[50], the critical R_g^{loop} for PS and P2VP is estimated to be 3.6 nm (with the segment length (a) of 0.67 nm[51]) from $R_g=(N/6)^{1/2}a$. Although the chain conformation in the direction normal to the surface is strongly collapsed compared to the bulk R_g for polymer

monolayer films[52], it is reasonable to suggest that the flattened layer, whose thickness is less than 3.6 nm, is not thick enough for entanglements with free chains in the top layer.

3.5 What happens if the thickness of the PS films become very small?

In the above discussions, the thickness of PS films were fixed to 20 nm, which in most of the cases ($M_w \leq 123$ kDa), are much larger than the unperturbed radius of gyration, R_g, in bulk. But what happens if the thickness of the PS films become much smaller. Figure 20 shows the surface morphology of 5 nm-thick PS films (M_w = 3.68 kDa and 123 kDa) prepared on bare H-Si substrate, PS flattened layer (Mw = 650 kDa) modified H-Si substrate and PS loosely adsorbed layer (Mw = 650 kDa) modified H-Si substrate after annealed at 150 ºC for 9 days.

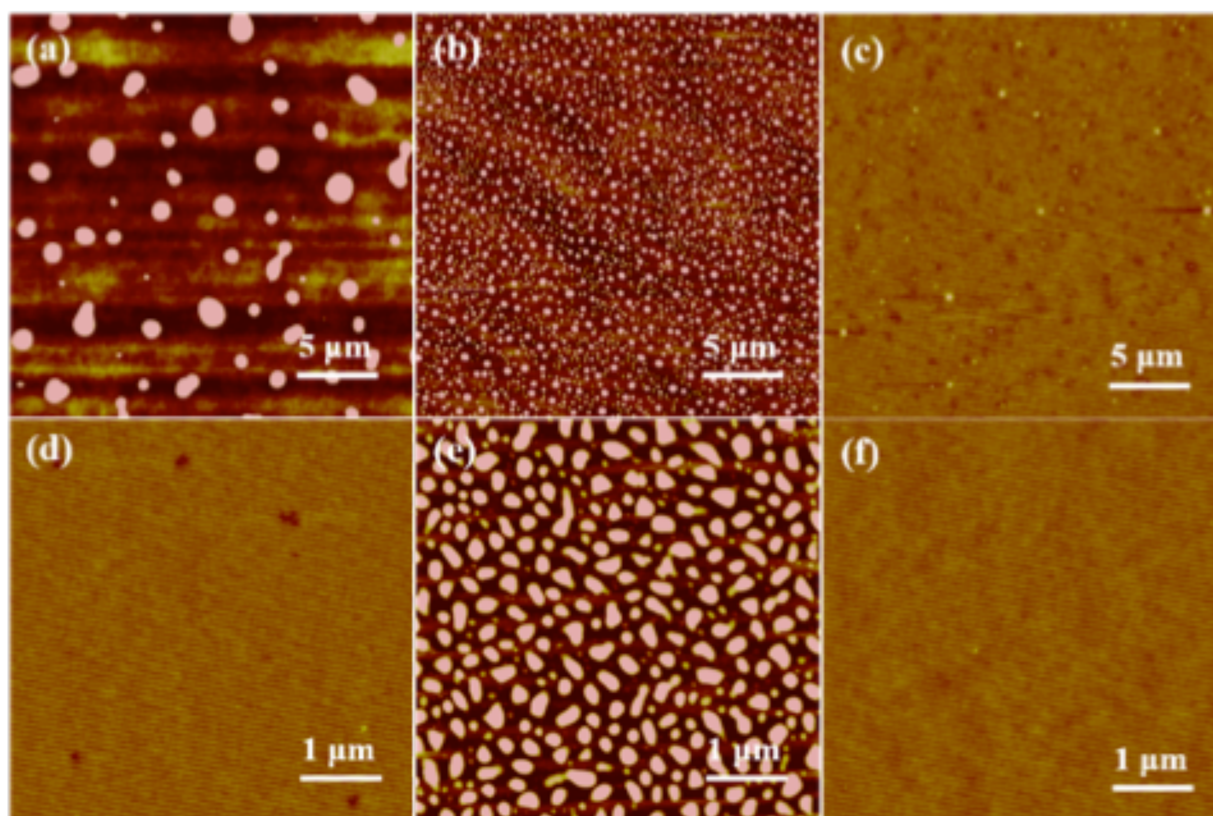

Figure 20. (a-c) shows AFM images of 5 nm-thick 3.68 kDa PS films on (a) bare H-Si substrate, (b) PS flattened layer (M_w = 650 kDa) modified H-Si substrate and (c) PS loosely

adsorbed layer (M_w = 650 kDa) modified H-Si substrate after thermally annealed at 150 ^oC under vacuum for 9 days. (d-f) shows AFM images of 5 nm-thick 123 kDa PS films on (d) bare H-Si substrate, (e) PS flattened layer (M_w = 650 kDa) modified H-Si substrate and (f) PS loosely adsorbed layer (M_w = 650 kDa) modified H-Si substrate after thermally annealed at 150 ^oC under vacuum for 9 days. The height scale for the AFM images is 0 – 20 nm.

As seen, both the average size of dewetting droplets and the average distance between neighboring droplets become much smaller compare to those 20 nm-thick PS film counterparts. For M_w = 3.68 kDa PS, the 5 nm-thick films also shows a large decrease in the average distance between neighboring droplets when they are prepared on the PS flattened layer modified H-Si substrates. At the same time, a numbers of initial formation of dewetting holes were found when the 3.68 kDa PS 5 nm-thick films were prepared on PS loosely adsorbed layer modified H-Si substrate and annealed for extremely long time.

On the other hand, when the 5 nm-thick 123 kDa PS films were prepared on bare H-Si substrate, a small amount of initial dewetting holes were formed (figure 20(d)), (but these holes do not further grow during the prolonged course of annealing). It should be noted that the original thickness of these 123 kDa PS film is almost the same as the thickness of the adsorbed layer formed within the 20 nm-thick 123 kDa PS films on H-Si substrate. After the toluene leaching process, the thickness of the 123 kDa PS residual film is found to be only 3.5 nm, indicating only partial of the 5 nm-thick film is transformed to the loosely adsorbed layer. This result indicate that when the thickness of the initial film is comparable or less than the required dimension of the loosely adsorbed layer, the formation of loosely adsorbed chains on the solid surface cannot be completed since the polymers are depleted at the interface. And the thinner, non-equilibrium

3.5 nm-thick adsorbed layer fails to stabilize the film strongly against dewetting. We also found that if the initial thickness of high M_w PS ($M_w \geq 123$ kDa) films is 3.5 nm, no loosely adsorbed layer is formed at the polymer-substrate interface. However, the 2 nm-thick flattened layer is always formed even when the initial film thickness is very thin. As a result, even when $M_w \geq 123$ kDa, dewetting can also be found once the film is not thick enough to form the loosely adsorbed layer on solid surfaces.

Comparing Figure 20 (d) - (f), it can be seen that on PS flattened layer modified H-Si substrate, the 5 nm-thick 123 kDa PS films become much easier to dewetting compare to the one prepared on bare H-Si substrate, while dewetting could be inhibited when the same films is prepared on PS loosely adsorbed layer modified H-Si substrate. After leaching the dewetted sample (Figure 20 (e)) with toluene, the thickness of the residual layer is only 2.4 nm, which almost the same as the original thickness of the PS flattened layer (2.1 nm-thick) on the modified H-Si substrate, but much thinner compare to the 3.5 nm-thick loosely adsorbed layer formed in 5 nm-thick 123 kDa PS films on H-Si substrate. Hence, there is no loosely adsorbed layer reformed at the polymer-solid interface. It is known that on a bare, unoccupied solid substrate, flattened layer and loosely adsorbed layer are formed simultaneously on the substrate. However, according to a series of bilayer studies, we found that the time for loosely adsorbed layer to form at the polymer-solid interface would become longer if there is a quasiequilibrium flattened layer already exist at the solid surface. This is likely due to the fact that an extra adsorption barrier is generated due to the presence of the final flattened chains. As a result, the free chains need more time to find the empty sites on the flattened layer modified solid surface. For 20 nm-thick PS films, loosely adsorbed layer is reformed on the flattened layer modified substrate before the film dewet.

However, for 5 nm-thick PS films, dewetting is already completed before any loosely adsorbed chains is reformed on the flattened layer modified substrate.

3.6 The mechanism of wetting/ dewetting of thin polymer films on silicon substrate.

By evidencing the different roles of the flattened chains (slippery) and the loosely adsorbed chains (non-slippery), we now rationalize the mechanism of wetting/dewetting of thin polymer films on silicon substrate. When the thin polymer film with thickness large than R_g is spun cast onto silicon substrates, the chains are trapped in a non-equilibrium state due to the rapid solvent evaporation[53]. It was also found that both the initial (non-equilibrium) flattened chains and loosely adsorbed chains emerge during the spin-casting process on the substrate surface [20, 54]. Previous study have shown that subsequent thermal annealing at $T>>T_g$ accelerates polymer adsorption, resulting in the equilibrated of both flattened layer and loosely adsorbed layer simultaneously at the polymer-solid interface. In case of PS, when the polymer chains are short (Mw $\leq$ 50 kDa), they only adsorbed with a flattened configuration at the polymer-substrate interface and there is no loosely adsorbed layer could be formed due to the short of chain length. The flattened chains have so many surface-segmental contacts with the substrate which makes them difficult to be effectively entangled or hooked with free chains. At the same time, the high density nature of flattened layer would generate negative excess interfacial entropy at the free polymer chains/flattened layer interface which makes the film even unstable. However, when the molecular weight is large enough (i.e. Mw $\geq$ 123 kDa in the present case), the loosely adsorbed polymer chains (i.e., loosely loops) are developed at the substrate interface along with the flattened chains, acting as connectors to stabilize the interface through the entanglements with free chains. The formation of loosely adsorbed chains and the subsequent interaction with unadsorbed chains generate an additional energy barrier against dewetting which may not be

overcome within experimental time scales. As a result, thin PS films with higher M_w ($M_w \geq 123$ kDa) prepared on bare silicon substrate are much difficult to dewet compared to those with lower M_w ($M_w \leq 50$ kDa), even the effective interfacial potential and spreading coefficient are the same. However, when the thickness of PS films become less than R_g or the size of the quasiequilibrium loosely adsorbed layer, dewetting may happen even for higher M_w ($M_w \geq 123$ kDa) PS due to the absence of loosely adsorbed chains at the polymer-solid interface.

The correlation between interfacial nano-architectures and film stability not only improve our understanding on the nature of dewetting of thin polymer films on solid substrate, but also enables us to effectively tune the thermal stability of thin polymer films by modify the silicon substrate with flattened layer or loosely adsorbed layer selectively, facilitating the development of novel nano-technological devices. To improve stabilization of small M_w ($M_w \leq 50$ kDa) PS films, we could modify the silicon substrate by pre-coating a loosely adsorbed layer using high M_w ($M_w \geq 123$ kDa) PS, as shown representatively in Figure 16 (f-i). Since we are only adding a chemically identical homopolymer nanolayer, the effective Hamaker constant A is expected to be the same, and consequently, the shape of the curve of the effective interface potential (φ) as a function of film thickness (h) should not change. Hence, dewetting inhibition mechanism with this approach is not considered as a thermodynamic mechanism, but a kinetic mechanism instead. Compare to the many other dewetting inhibition approaches, including cross-linking the polymer films [55], adding block copolymers, dendrimers, nanoparticles or other component to the film [56-61], chemical and physical modifications of the substrate [62, 63], grafting homopolymer brush [34, 64-68] or block copolymer[69], and the introducing of specialized end groups onto the polymer [70, 71], the use of loosely adsorbed nanolayer is the most easiest and efficiently way to prevent dewetting without largely change the chemical composition of the film. On the other hand, the stabilization

of a non-dewetting polymer/solid system can be easily deteriorated by pre-coating a flattened layer on the solid surface. Even when the flattened layer is heterogeneous due to weak interaction, i.e. in case of PS on silicon, destabilization of the a high Mw PS film can also be achieved when the film thickness is small enough. In these cases, competition between dewetting and the “reel in” process of unadsorbed chains plays a crucial role and dewetting would be strongly suppressed once loosely adsorbed chains are reformed and become stabilized at the available empty spaces on the solid surface.

Chapter 4. Conclusion

In conclusion, we have found the strong correlation between macroscopic film stability of liquid polymer films and microscopic chain adsorption at the polymer-solid interface. The key is the formation of the nano-architectures of the adsorbed polymer chains before the dewetting is thermally induced: the flattened chains are non-wetting even against chemically identical polymers, while the loosely adsorbed chains allows the penetration of the chemically identical polymer with wide range of molecular weights (3.68 kDa $\leq M_w \leq$ 650 kDa) into them. Since such adsorbed nanolayers are composed of the chemically identical polymer, the shape of the effective interface potential curve as a function of the thickness of the PS liquid films remain unchanged compared to that for the air/PS/SiOx/Si system. Hence, the mechanism of the dewetting inhibition in the present study is not considered as a thermodynamic mechanism, but a kinetic mechanism. These novel features would allow us to utilize the adsorbed polymer nanolayers as new polymer coating materials in place of conventional chemically end-grafted polymer chains. Compared to the chemical end-grafting approaches, the film preparation of the adsorbed nanolayers is simple (i.e., no sophisticated chemistry is involved). In addition, due to many solid-segment contacts, the adsorbed nanolayers are stable against high temperature and solvents. Furthermore, additional processing steps, such as crosslinking or inclusion of nanoparticles are required to control wetting/non-wetting properties of liquid films on top. At the same time, we found the present concept of film stabilization at the (adsorbed) polymer- (melt) polymer interface is applicable to P2VP/SiOx/Si that has very strong affinity between the polymer and substrate. Hence, the present results open up a new strategy to stabilize non-wetting liquid films on solids by using non-functionalized commodity homopolymers.

References

1. Reiter, G. *Physical Review Letters* **1992,** 68, (1), 75-78.

2. Reiter, G.; Sharma, A.; Casoli, A.; David, M.-O.; Khanna, R.; Auroy, P. *Langmuir* **1999,** 15, (7), 2551-2558.

3. Sharma, A. *Langmuir* **1993,** 9, (3), 861-869.

4. Reiter, G. *EPL (Europhysics Letters)* **1993,** 23, (8), 579.

5. Reiter, G. *Physical Review Letters* **2001,** 87, (18), 186101.

6. Ralf, S.; Stephan, H.; Chiara, N.; Stefan, S.; Daniel, P.; Renate, K.; Hubert, M.; Karin, J. *Journal of Physics: Condensed Matter* **2005,** 17, (9), S267.

7. Reiter, G. *Langmuir* **1993,** 9, (5), 1344-1351.

8. Sharma, A.; Reiter, G. *Journal of Colloid and Interface Science* **1996,** 178, (2), 383-399.

9. Ashley, K. M.; Raghavan, D.; Douglas, J. F.; Karim, A. *Langmuir* **2005,** 21, (21), 9518-9523.

10. Reiter, G., Visualizing Properties of Polymers at Interfaces. In *Soft Matter Characterization*, Borsali, R.; Pecora, R., Eds. Springer Netherlands: 2008; pp 1243-1292.

11. Seemann, R.; Herminghaus, S.; Jacobs, K. *Physical Review Letters* **2001,** 86, (24), 5534-5537.

12. Karin, J.; Ralf, S.; Stephan, H., STABILITY AND DEWETTING OF THIN LIQUID FILMS. In *Polymer Thin Films*, WORLD SCIENTIFIC: 2008; Vol. Volume 1, pp 243-265.

13. Xue, L.; Han, Y. *Progress in Polymer Science* **2011,** 36, (2), 269-293.

14. Becker, J.; Grun, G.; Seemann, R.; Mantz, H.; Jacobs, K.; Mecke, K. R.; Blossey, R. *Nat Mater* **2003,** 2, (1), 59-63.

15. Chen, Y. L.; Chen, S.; Frank, C.; Israelachvili, J. *Journal of Colloid and Interface Science* **1992,** 153, (1), 244-265.

16. Fujii, Y.; Yang, Z. H.; Leach, J.; Atarashi, H.; Tanaka, K.; Tsui, O. K. C. *Macromolecules* **2009,** 42, (19), 7418-7422.

17. Napolitano, S.; Wubbenhorst, M. *Nat Commun* **2011,** 2.

18. Koga, T.; Jiang, N.; Gin, P.; Endoh, M. K.; Narayanan, S.; Lurio, L. B.; Sinha, S. K. *Phys Rev Lett* **2011,** 107, (22).

19. Asada, M.; Jiang, N.; Sendogdular, L.; Gin, P.; Wang, Y.; Endoh, M. K.; Koga, T.; Fukuto, M.; Schultz, D.; Lee, M.; Li, X.; Wang, J.; Kikuchi, M.; Takahara, A. *Macromolecules* **2012,** 45, (17), 7098-7106.

20. Jiang, N.; Shang, J.; Di, X.; Endoh, M. K.; Koga, T. *Macromolecules* **2014,** 47, (8), 2682-2689.

21. Asada, M.; Jiang, N.; Sendogdular, L.; Sokolov, J.; Endoh, M. K.; Koga, T.; Fukuto, M.; Yang, L.; Akgun, B.; Dimitriou, M.; Satija, S. *Soft Matter* **2014,** 10, (34), 6392-6403.

22. Gin, P.; Jiang, N.; Liang, C.; Taniguchi, T.; Akgun, B.; Satija, S. K.; Endoh, M. K.; Koga, T. *Physical Review Letters* **2012,** 109, (26), 265501.

23. Napolitano, S.; Pilleri, A.; Rolla, P.; Wübbenhorst, M. *Acs Nano* **2010,** 4, (2), 841-848.

24. Napolitano, S.; Lupascu, V.; Wubbenhorst, M. *Macromolecules* **2008,** 41, (4), 1061-1063.

25. Napolitano, S.; Wubbenhorst, M. *J Phys Chem B* **2007,** 111, (31), 9197-9199.

26. Vanroy, B.; Wübbenhorst, M.; Napolitano, S. *Acs Macro Lett* **2013,** 2, (2), 168-172.

27. Jiang, N.; Endoh, M. K.; Koga, T. *Polym J* **2013,** 45, (1), 26-33.

28. Douglas, J. F.; Schneider, H. M.; Frantz, P.; Lipman, R.; Granick, S. *Journal of Physics: Condensed Matter* **1997,** 9, (37), 7699.

29. O'Shaughnessy, B.; Vavylonis, D. *Physical Review Letters* **2003,** 90, (5), 056103.

30. O'Shaughnessy, B.; Vavylonis, D. *Eur Phys J E* **2003,** 11, (3), 213-230.

31. Koga, T.; Jiang, N.; Gin, P.; Endoh, M. K.; Narayanan, S.; Lurio, L. B.; Sinha, S. K. *Physical Review Letters* **2011,** 107, (22), 225901.

32. Qu, S.; Clarke, C. J.; Liu, Y.; Rafailovich, M. H.; Sokolov, J.; Phelan, K. C.; Krausch, G. *Macromolecules* **1997,** 30, (12), 3640-3645.

33. Wang, C.; Krausch, G.; Geoghegan, M. *Langmuir* **2001,** 17, (20), 6269-6274.

34. Reiter, G.; Auroy, P.; Auvray, L. *Macromolecules* **1996,** 29, (6), 2150-2157.

35. Maas, J. H.; Fleer, G. J.; Leermakers, F. A. M.; Cohen Stuart, M. A. *Langmuir* **2002,** 18, (23), 8871-8880.

36. Voronov, A.; Shafranska, O. *Langmuir* **2002,** 18, (11), 4471-4477.

37. Fujii, Y.; Yang, Z.; Leach, J.; Atarashi, H.; Tanaka, K.; Tsui, O. K. C. *Macromolecules* **2009,** 42, (19), 7418-7422.

38. Napolitano, S.; Wubbenhorst, M. *Nat Commun* **2011,** 2, 260.

39. Shin, K.; Hu, X.; Zheng, X.; Rafailovich, M. H.; Sokolov, J.; Zaitsev, V.; Schwarz, S. A. *Macromolecules* **2001,** 34, (14), 4993-4998.

40. Müller-Buschbaum, P. *Eur. Phys. J. E* **2003,** 12, (3), 443-448.

41. Reiter, G.; Schultz, J.; Auroy, P.; Auvray, L. *EPL (Europhysics Letters)* **1996,** 33, (1), 29.

42. Huang, Z.; Ji, H.; Mays, J. W.; Dadmun, M. D. *Macromolecules* **2008,** 41, (3), 1009-1018.

43. Patton, D.; Knoll, W.; Advincula, R. C. *Macromolecular Chemistry and Physics* **2011,** 212, (5), 485-497.

44. De Gennes, P.-G., *Scaling concepts in polymer physics*. Cornell university press: 1979.

45. Dadmun, M. *Macromolecules* **1996,** 29, (11), 3868-3874.

46. Eastwood, E. A.; Dadmun, M. D. *Macromolecules* **2002,** 35, (13), 5069-5077.

47. Reiter, G.; Khanna, R. *Phys Rev Lett* **2000,** 85, (26), 5599-5602.

48. Leibler, L.; Ajdari, A.; Mourran, A.; Coulon, G.; Chatenay, D., Wetting of Grafted Polymer Surfaces by Compatible Chains. In *Ordering in Macromolecular Systems*, Teramoto, A.; Kobayashi, M.; Norisuye, T., Eds. Springer Berlin Heidelberg: 1994; pp 301-311.

49. Shull, K. R. *Faraday Discussions* **1994,** 98, 203-217.

50. Creton, C.; Kramer, E. J.; Hadziioannou, G. *Macromolecules* **1991,** 24, (8), 1846-1853.

51. Park, C. H.; Kim, J. H.; Ree, M.; Sohn, B.-H.; Jung, J. C.; Zin, W.-C. *Polymer* **2004,** 45, (13), 4507-4513.

52. Soles, C. L.; Ding, Y. *Science* **2008,** 322, (5902), 689-690.

53. Thomas, K. R.; Chenneviere, A.; Reiter, G.; Steiner, U. *Phys Rev E* **2011,** 83, (2), 021804.

54. Durning, C. J.; O'Shaughness, B.; Sawhney, U.; Nguyen, D.; Majewski, J.; Smith, G. S. *Macromolecules* **1999,** 32, (20), 6772-6781.

55. Carroll, G. T.; Sojka, M. E.; Lei, X. G.; Turro, N. J.; Koberstein, J. T. *Langmuir* **2006,** 22, (18), 7748-7754.

56. Kropka, J. M.; Green, P. F. *Macromolecules* **2006,** 39, (25), 8758-8762.

57. Costa, A. C.; Composto, R. J.; Vlcek, P. *Macromolecules* **2003,** 36, (9), 3254-3260.

58. Oslanec, R.; Costa, A. C.; Composto, R. J.; Vlcek, P. *Macromolecules* **2000,** 33, (15), 5505-5512.

59. Barnes, K. A.; Karim, A.; Douglas, J. F.; Nakatani, A. I.; Gruell, H.; Amis, E. J. *Macromolecules* **2000,** 33, (11), 4177-4185.

60. Mackay, M. E.; Hong, Y.; Jeong, M.; Hong, S.; Russell, T. P.; Hawker, C. J.; Vestberg, R.; Douglas, J. F. *Langmuir* **2002,** 18, (5), 1877-1882.

61. Krishnan, R. S.; Mackay, M. E.; Hawker, C. J.; Van Horn, B. *Langmuir* **2005,** 21, (13), 5770-5776.

62. Kargupta, K.; Sharma, A. *Langmuir* **2002,** 18, (5), 1893-1903.

63. Kargupta, K.; Konnur, R.; Sharma, A. *Langmuir* **2000,** 16, (26), 10243-10253.

64. Yerushalmi-Rozen, R.; Klein, J.; Fetters, L. J. *Science* **1994,** 263, (5148), 793-795.

65. Yerushalmi-Rozen, R.; Klein, J. *Langmuir* **1995,** 11, (7), 2806-2814.

66. Rachel, Y.-R.; Jacob, K. *Journal of Physics: Condensed Matter* **1997,** 9, (37), 7753.

67. Reiter, G.; Schultz, J.; Auroy, P.; Auvray, L. *Europhys Lett* **1996,** 33, (1), 29-34.

68. Voronov, A.; Shafranska, O. *Langmuir* **2002,** 18, (11), 4471-4477.

69. Liu, Y.; Rafailovich, M. H.; Sokolov, J.; Schwarz, S. A.; Zhong, X.; Eisenberg, A.; Kramer, E. J.; Sauer, B. B.; Satija, S. *Phys Rev Lett* **1994,** 73, (3), 440-443.

70. Henn, G.; Bucknall, D. G.; Stamm, M.; Vanhoorne, P.; Jerome, R. *Macromolecules* **1996,** 29, (12), 4305-4313.

71. Feng, Y.; Karim, A.; Weiss, R. A.; Douglas, J. F.; Han, C. C. *Macromolecules* **1998,** 31, (2), 484-493.